non-Treg cells was not significantly changed in the colon and spleen of mice maintained with vitamin B9(−) diet (Fig. 5C), which could be explained by the similar concentration of vitamin B9 in the large-intestinal washes and sera of both groups of mice. We also found that Foxp3 and the inhibitory molecules CTLA4 and GITR, which are specifically expressed on Treg cells, were comparable between those mice (Fig. 5D).

Discussion

We have shown that vitamin B9 is crucial for the maintenance of Treg cells. Intriguingly, vitamin B9 was required for the survival of differentiated Treg cells, but was not necessary for the differentiation of naïve T cells into Treg cells. This selective effect of vitamin B9 on Treg cells is opposite to the effect of RA, a vitamin A metabolite, which enhances the differentiation of naïve T cells into Treg cells [11,12,13,14]. RA also induces the expression of gut-homing molecules (e.g., $\alpha4\beta7$ integrin and CCR9) on B and T cells activated by gut dendritic cells [9,10]. Because CCR9 was expressed normally on Treg cells in the LP of mice maintained with vitamin B9(−) diet (data not shown), the deficiency of dietary vitamin B9 did not affect the RA-mediated expression of gut-homing molecules and, predictably, the induction of Treg cells in the small intestine.

Treatment with the vitamin B9 antagonist MTX affected survival of both Treg cells and non-Treg cells, suggesting that the carrier-mediated pathway maintains sufficient amounts of intracellular vitamin B9 for cell survival regardless of the T-cell subset. The indiscriminate effects of MTX could be explained by the ubiquitous expression of the folate carrier [29,34]. As the mechanism of FR4-mediated Treg-cell maintenance, we considered initially that the proliferative activity of Treg cells could require large amounts of vitamin B9 as a source of nucleotides for DNA and RNA. However, the amounts of intracellular vitamin B9 were identical between Treg and non-Treg cells, implying that FR4 specifically recognizes extracellular vitamin B9 for the maintenance of Treg cell survival, consistent with a report that FR4 expressed on Treg cells contributes to their immune function and survival [25]. Additionally, the specific biological functions of vitamin B9 receptors (FR1, FR2, and FR4) have been predicted on the basis of their ~70% amino acid sequence identity, but the expression of each receptor is rigidly restricted, with narrow tissue and cell specificity [35,36]. Because FR1, FR2, and FR4 are glycosyl phosphatidylinositol–anchored proteins [37], adapter molecules may assist FR4 in the maintenance of Treg cell survival. We found that vitamin B9/FR4 was not associated with IL-2–mediated signaling in Treg cells. We will continue to study how FR4-mediated vitamin B9 regulates the survival of Treg cells.

Mammals must obtain vitamin B9 from the diet or from commensal bacteria. The absorption of vitamin B9 from the diet occurs mainly in the small intestine, whereas the uptake of microbial vitamin B9 predominantly occurs in the colon [38]. This explains why depletion of dietary vitamin B9 specifically decreased Treg cells in the small intestine, but not in the colon. It has been proposed that bacterial vitamin B9 absorbed in the colon affects the vitamin B9 status of the host [39,40], which may explain the lack of changes in vitamin B9 in the serum and splenic Treg cells in mice maintained with vitamin B9(−) diet. *Bifidobacterium*, one of the most important genera of commensal bacteria to be used as a probiotic, is well-studied as a vitamin B9 producer [41], and colonic Treg cells are specifically induced by immunological crosstalk with commensal bacteria, especially *Clostridium* clusters IV and XIVa [5]. Although whether *Clostridium* clusters IV and XIVa produce vitamin B9 remains unclear, our current findings suggest that vitamin B9 is an essential survival factor for Treg cells and, in vivo situation, diet vitamin B9 establishes an immunological network in the maintenance of Treg cells specifically in the small intestine.

Acknowledgments

We thank Drs. K. Takeda and M. Kinoshita (Osaka University) for their constructive discussions and Mr. Y. Suzuki, Mrs. S. Shikata, and Mrs. R. Sumiya (University of Tokyo) for technical supports.

Author Contributions

Conceived and designed the experiments: JK. Performed the experiments: JK EH II. Analyzed the data: JK EH II. Wrote the paper: JK HK.

References

1. Kiyono H, Kunisawa J, McGhee JR, Mestecky J (2008) The mucosal immune system. In: Paul WE, ed. Fundamental Immunology. Philadelphia: Lippincott-Raven. pp 983–1030.
2. Littman DR, Rudensky AY (2010) Th17 and regulatory T cells in mediating and restraining inflammation. Cell 140: 845–858.
3. Cebra JJ, Jiang HQ, Boiko NV, Tlaskalva-Hogenova H (2005) The role of mucosal microbiota in the development, maintenance, and pathologies of the mucosal immune system. In: Mestecky J, Lamm ME, Strober W, Bienenstock J, McGhee JR, et al., eds. Mucosal Immunology. 3rd ed. San Diego: Academic Press. pp 335–368.
4. Ivanov II, Atarashi K, Manel N, Brodie EL, Shima T, et al. (2009) Induction of intestinal Th17 cells by segmented filamentous bacteria. Cell 139: 485–498.
5. Atarashi K, Tanoue T, Shima T, Imaoka A, Kuwahara T, et al. (2011) Induction of colonic regulatory T cells by indigenous Clostridium species. Science 331: 337–341.
6. Geuking MB, Cahenzli J, Lawson MA, Ng DC, Slack E, et al. (2011) Intestinal bacterial colonization induces mutualistic regulatory T cell responses. Immunity 34: 794–806.
7. Hanson LA, Robertson A, Bjersing J, Herias MV (2005) Undernutrition, Immunodeficiency, and Mucosal Infections. In: Mestecky J, Lamm ME, Strober W, Bienenstock J, McGhee JR, et al., eds. Mucosal Immunology. 3rd ed. San Diego: Academic Press. pp 1159–1178.
8. Wintergerst ES, Maggini S, Hornig DH (2007) Contribution of selected vitamins and trace elements to immune function. Ann Nutr Metab 51: 301–323.
9. Iwata M, Hirakiyama A, Eshima Y, Kagechika H, Kato C, et al. (2004) Retinoic acid imprints gut-homing specificity on T cells. Immunity 21: 527–538.
10. Mora JR, Iwata M, Eksteen B, Song SY, Junt T, et al. (2006) Generation of gut-homing IgA-secreting B cells by intestinal dendritic cells. Science 314: 1157–1160.
11. Coombes JL, Siddiqui KR, Arancibia-Carcamo CV, Hall J, Sun CM, et al. (2007) A functionally specialized population of mucosal $CD103^+$ DCs induces $Foxp3^+$ regulatory T cells via a TGF-β and retinoic acid-dependent mechanism. J Exp Med 204: 1757–1764.
12. Sun CM, Hall JA, Blank RB, Bouladoux N, Oukka M, et al. (2007) Small intestine lamina propria dendritic cells promote de novo generation of Foxp3 Treg cells via retinoic acid. J Exp Med 204: 1775–1785.
13. Benson MJ, Pino-Lagos K, Rosemblatt M, Noelle RJ (2007) All-trans retinoic acid mediates enhanced T reg cell growth, differentiation, and gut homing in the face of high levels of co-stimulation. J Exp Med 204: 1765–1774.
14. Mucida D, Park Y, Kim G, Turovskaya O, Scott I, et al. (2007) Reciprocal Th17 and regulatory T cell differentiation mediated by retinoic acid. Science 317: 256–260.
15. Rivera J, Proia RL, Olivera A (2008) The alliance of sphingosine-1-phosphate and its receptors in immunity. Nat Rev Immunol 8: 753–763.
16. Miller LT, Kerkvliet NI (1990) Effect of vitamin B6 on immunocompetence in the elderly. Ann N Y Acad Sci 587: 49–54.
17. Schwab SR, Pereira JP, Matloubian M, Xu Y, Huang Y, et al. (2005) Lymphocyte sequestration through S1P lyase inhibition and disruption of S1P gradients. Science 309: 1735–1739.
18. Kunisawa J, Kurashima Y, Higuchi M, Gohda M, Ishikawa I, et al. (2007) Sphingosine 1-phosphate dependence in the regulation of lymphocyte trafficking to the gut epithelium. J Exp Med 204: 2335–2348.
19. Iyer R, Tomar SK (2009) Folate: a functional food constituent. J Food Sci 74: R114–122.
20. Stover PJ (2004) Physiology of folate and vitamin B12 in health and disease. Nutr Rev 62: S3–12. discussion S13.
21. Gangjee A, Jain HD, Kurup S (2008) Recent advances in classical and non-classical antifolates as antitumor and antiopportunistic infection agents: Part II. Anticancer Agents Med Chem 8: 205–231.
22. Bourre-Tessier J, Haraoui B (2010) Methotrexate drug interactions in the treatment of rheumatoid arthritis: a systematic review. J Rheumatol 37: 1416–1421.

23. Courtemanche C, Elson-Schwab I, Mashiyama ST, Kerry N, Ames BN (2004) Folate deficiency inhibits the proliferation of primary human $CD8^+$ T lymphocytes in vitro. J Immunol 173: 3186–3192.
24. Troen AM, Mitchell B, Sorensen B, Wener MH, Johnston A, et al. (2006) Unmetabolized folic acid in plasma is associated with reduced natural killer cell cytotoxicity among postmenopausal women. J Nutr 136: 189–194.
25. Yamaguchi T, Hirota K, Nagahama K, Ohkawa K, Takahashi T, et al. (2007) Control of immune responses by antigen-specific regulatory T cells expressing the folate receptor. Immunity 27: 145–159.
26. Gohda M, Kunisawa J, Miura F, Kagiyama Y, Kurashima Y, et al. (2008) Sphingosine 1-phosphate regulates the egress of IgA plasmablasts from Peyer's patches for intestinal IgA responses. J Immunol 180: 5335–5343.
27. Zhao R, Matherly LH, Goldman ID (2009) Membrane transporters and folate homeostasis: intestinal absorption and transport into systemic compartments and tissues. Expert Rev Mol Med 11: e4.
28. Jansen G, Westerhof GR, Jarmuszewski MJ, Kathmann I, Rijksen G, et al. (1990) Methotrexate transport in variant human CCRF-CEM leukemia cells with elevated levels of the reduced folate carrier. Selective effect on carrier-mediated transport of physiological concentrations of reduced folates. J Biol Chem 265: 18272–18277.
29. Biswal BK, Verma RS (2009) Differential usage of the transport systems for folic acid and methotrexate in normal human T-lymphocytes and leukemic cells. J Biochem 146: 693–703.
30. Takahashi T, Kuniyasu Y, Toda M, Sakaguchi N, Itoh M, et al. (1998) Immunologic self-tolerance maintained by $CD25^+CD4^+$ naturally anergic and suppressive T cells: induction of autoimmune disease by breaking their anergic/suppressive state. Int Immunol 10: 1969–1980.
31. Setoguchi R, Hori S, Takahashi T, Sakaguchi S (2005) Homeostatic maintenance of natural $Foxp3^+$ $CD25^+$ $CD4^+$ regulatory T cells by interleukin (IL)-2 and induction of autoimmune disease by IL-2 neutralization. J Exp Med 201: 723–735.
32. D'Cruz LM, Klein L (2005) Development and function of agonist-induced $CD25^+Foxp3^+$ regulatory T cells in the absence of interleukin 2 signaling. Nat Immunol 6: 1152–1159.
33. Fontenot JD, Rasmussen JP, Gavin MA, Rudensky AY (2005) A function for interleukin 2 in Foxp3-expressing regulatory T cells. Nat Immunol 6: 1142–1151.
34. Matherly LH, Hou Z, Deng Y (2007) Human reduced folate carrier: translation of basic biology to cancer etiology and therapy. Cancer Metastasis Rev 26: 111–128.
35. Salazar MD, Ratnam M (2007) The folate receptor: what does it promise in tissue-targeted therapeutics? Cancer Metastasis Rev 26: 141–152.
36. Low PS, Kularatne SA (2009) Folate-targeted therapeutic and imaging agents for cancer. Curr Opin Chem Biol 13: 256–262.
37. Jia Z, Zhao R, Tian Y, Huang Z, Tian Z, et al. (2009) A novel splice variant of FR4 predominantly expressed in $CD4^+CD25^+$ regulatory T cells. Immunol Invest 38: 718–729.
38. Said HM, Mohammed ZM (2006) Intestinal absorption of water-soluble vitamins: an update. Curr Opin Gastroenterol 22: 140–146.
39. Aufreiter S, Gregory JF, 3rd, Pfeiffer CM, Fazili Z, Kim YI, et al. (2009) Folate is absorbed across the colon of adults: evidence from cecal infusion of (13)C-labeled [6S]-5-formyltetrahydrofolic acid. Am J Clin Nutr 90: 116–123.
40. Said HM (2011) Intestinal absorption of water-soluble vitamins in health and disease. Biochem J 437: 357–372.
41. Pompei A, Cordisco L, Amaretti A, Zanoni S, Matteuzzi D, et al. (2007) Folate production by bifidobacteria as a potential probiotic property. Appl Environ Microbiol 73: 179–185.

Bioconjugate Chemistry

ARTICLE

pubs.acs.org/bc

New Protein Purification System Using Gold-Magnetic Beads and a Novel Peptide Tag, "the Methionine Tag"

Yoshiaki Okada,[*,#,†] Tomoko Y. Takano,[#,†] Nozomi Kobayashi,[†] Arisa Hayashi,[†] Masaaki Yonekura,[†] Yuji Nishiyama,[†] Tomohiro Abe,[†] Takuya Yoshida,[†] Takao A. Yamamoto,[‡] Satoshi Seino,[‡] and Takefumi Doi[†]

[†]Graduate School of Pharmaceutical Sciences, Osaka University

[‡]Graduate School of Engineering, Osaka University

Supporting Information

ABSTRACT: Gold magnetic particles (GMP) are magnetic iron oxide particles modified with gold nanoparticles. The gold particles of GMP specifically bind to cysteine and methionine through Au−S binding. The aim of the present study was to establish a quick and easy protein purification system using novel peptide tags and GMP. Here, we created a variety of peptide tags containing methionine and cysteine and analyzed their affinity to GMP. Binding assays using enhanced green fluorescent protein (EGFP) as a model protein indicated that the tandem methionine tags comprising methionine residues had higher affinity to the GMP than tags comprising both methionine and cysteine residues. Tags comprising both methionine and glycine residues showed slightly higher affinity to GMP and higher elution efficiency than the all-methionine tags. A protein purification assay using phosphorylcholine-treated GMP demonstrated that both a tandem methionine-tagged EGFP and a methionine and glycine-tagged EGFP were specifically purified from a protein mixture with very high efficiency. The efficiency was comparable to that of a histidine-tagged protein purification system. Together, these novel peptide tags, "methionine tags", specifically bind to GMP and can be used for a highly efficient protein purification system.

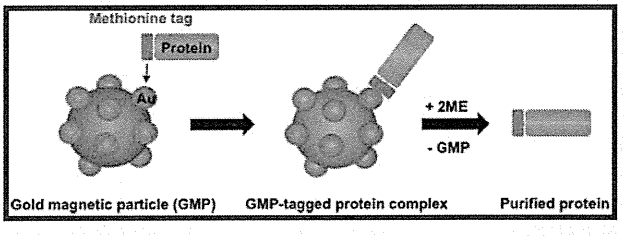

INTRODUCTION

Protein purification using ion exchange, gel filtration, and affinity chromatography is commonly used to study protein function. Affinity chromatography is a powerful tool to purify a target protein by single column chromatography. Several protein and peptide tags are used for affinity chromatography such as glutathione S-transferase,[1] maltose-binding protein,[2,3] FLAG-tag,[4] hexahistidine tag,[5,6] calmodulin-binding peptide,[7] biotin acceptor peptide,[8] and strep-tag.[1,9] Each of these tags is fused to the target protein, and the tagged protein is purified using chemically modified beads with high affinity to the tag.

Magnet beads are used for protein purification. Because magnet beads in solution are easily collected with a magnet, these beads are used as biologic research tools for molecular interaction analysis, nucleic acid/protein purification in gene delivery,[10] cell separation,[11,12] tumor targeting,[13] magnetic resonance imaging,[14,15] and hyperthermic cancer therapy.[16,17] In most cases, chemically modified magnetic beads are used to immobilize a molecule (e.g., protein or DNA molecule) on the bead surface.[18]

The gold magnetic particle (GMP) is a novel magnetic bead on which nanoscale gold particles are immobilized.[19,20] Molecules including sulfur atoms (thiol sulfide and disulfide groups) bind to GMP through Au−S binding without the need for chemical linkers.[21,22] Only amino acids with sulfur atoms, such as cysteine and methionine residues, specifically bind to GMP.[23] In the present study, we developed novel peptide tags that strongly and specifically bind to GMP and successfully established a novel efficient protein purification system using these tags and GMP.

EXPERIMENTAL PROCEDURES

Preparation of Gold Magnetic Particle. Gold magnetic particles (GMP) were synthesized as previously described.[24] Briefly, 20 to 30 nm Fe_3O_4 nanoparticles (Nanostructured & Amorphous Materials, Inc., Houston, TX) were dispersed in water containing 0.5 mM $HAuCl_4$, 125 mM 2-propanol, and 1 mg/mL poly(vinyl pyrrolidone) (molecular weight 40 k) to prepare a 0.1 mg/mL Fe_3O_4 suspension. This suspension was irradiated with a 4.8 MeV high-energy electron beam at a dose rate of 3k Gy/s for 2 s in a glass vial. The resulting Au/Fe_3O_4 nanoparticles were collected with a magnet, washed with water three times, and resuspended in water. Production of Au/Fe_3O_4 particles containing 2 to 4 nm Au particles immobilized on the surface of Fe_3O_4 particles was confirmed by transmission electron microscopy. GMPs are now commercially available (Act Nonpareil, Osaka, Japan; URL: http://www.act-nonpareil.com/en/).

Received: September 29, 2010
Revised: February 17, 2011
Published: April 13, 2011

To generate GMP-PC, gold magnetic particles were treated with phosphorylcholine.

Construction of Expression Vectors. Each tandem methionine tag was fused to enhanced green fluorescent proteins (EGFP) by a polypeptide linker that includes a protease recognition site, a helix linker, and a tag sequence (Supporting Information Figure S1). To generate pET-15b-EGFP-linker-MMM, a DNA fragment encoding the linker and the tandem methionine tag was generated by annealing several oligonucleotides. This fragment was cloned into *Eco*RI and *Bgl*II sites of pCruz-GFP (Santa Cruz Biotechnology, Santa Cruz, CA) (Supporting Information Figures S2 and S3). pCruz-EGFP-linker-MMM was then digested with *Nco*I and *Bgl*II, and the resulting fragment encoding EGFP-linker-MMM was inserted into the *Nco*I and *Bam*HI sites of pET-15b (Merck KGaA, Darmstadt, Germany) (Supporting Information Figure S3).

To generate the other tagged EGFP expression vectors, oligonucleotides encoding the tag sequences were cloned into *Not*I and *Sac*II sites of pCruz-EGFP-linker-MMM (Supporting Information Figure S2). The resulting plasmids were digested with *Nco*I and *Bgl*II, and the resulting fragments encoding the EGFP-linker-tag were inserted into the *Nco*I and *Bam*HI sites of pET-15b. The DNA sequences of each of the constructs were verified by automated DNA sequencing.

To generate pET-15b-CBFβ-linker-M3G4, a DNA fragment encoding CBFβ and a part of the polypeptide linker sequence was amplified by PCR. The resulting PCR product was digested with *Nco*I and *Sma*I, and cloned into the *Nco*I and *Sma*I sites of pET-15b-EGFP-linker-M3G4.

Preparation of the Tagged EGFPs. To prepare the tagged EGFPs, each of expression vectors for the tagged EGFP was transfected into *E. coli* strain BL21(DE3). The resulting *E. coli* were cultured in Luria–Bertani medium containing 50 μg/mL carbenicillin. When the OD_{600} reached 0.3, isopropyl β-D-thiogalactoside was added to a final concentration of 1 mM to induce the tagged EGFP. The cells were incubated for another 3 h at 30 °C and harvested. The cells were washed twice and resuspended with Buffer I (20 mM Tris-HCl [pH 8.0], 50 mM NaCl, 1 mM dithiothreitol (DTT), and protease inhibitor cocktail [Nacalai Tesque, Kyoto, Japan]). The resulting cell suspension was sonicated to extract and resolve the tagged EGFP. To purify the tagged proteins, the cell extract was applied to an Econo pack High Q cartridge (Bio-Rad, Hercules, CA). The column was then washed with Buffer II (20 mM Tris-HCl [pH 8.0], 80 mM NaCl, 1 mM DTT) and eluted with an 80–110 mM NaCl linear gradient. Fractions containing the tagged EGFP were collected and concentrated using Vivaspin 20 cartridges (Sartorius Stedim Biotech, Aubagne, France). The fluorescence intensity of the purified, tagged EGFP was measured using Gemini XPS (Molecular Devices, Sunnyvale, CA).

Protein Binding/Purification Assay and Sodium Dodecyl Sulfate-Polyacrylamide Gel Electrophoresis (SDS-PAGE) Analysis. For the protein binding assay, 15 000 fluorescence units of the tagged protein was mixed with GMP containing 10 mg iron in 300 μL of binding buffer (20 mM Tris-HCl [pH 8.0], 100 mM NaCl) and incubated for 30 min at 4 °C. The GMP in the resulting solution was collected with a magnet, and the fluorescence intensity of the supernatant was measured. The collected GMP was washed twice with binding buffer and incubated in 300 μL of binding buffer containing 24 mM 2-mercaptoethanol (2-ME) following for 30 min at 4 °C. The fluorescence intensity of the eluted proteins was measured. The same procedure was used for the protein purification assay with nonpurified *E. coli* extract containing 15 000 fluorescence units of the tagged EGFPs. For the protein purification assay using histidine tagged EGFP, Dynabeads TALON (Invitrogen, Carlsbad, CA) was used. Crude protein extract and eluted protein were subjected to SDS-PAGE following Coomassie Brilliant Blue staining.

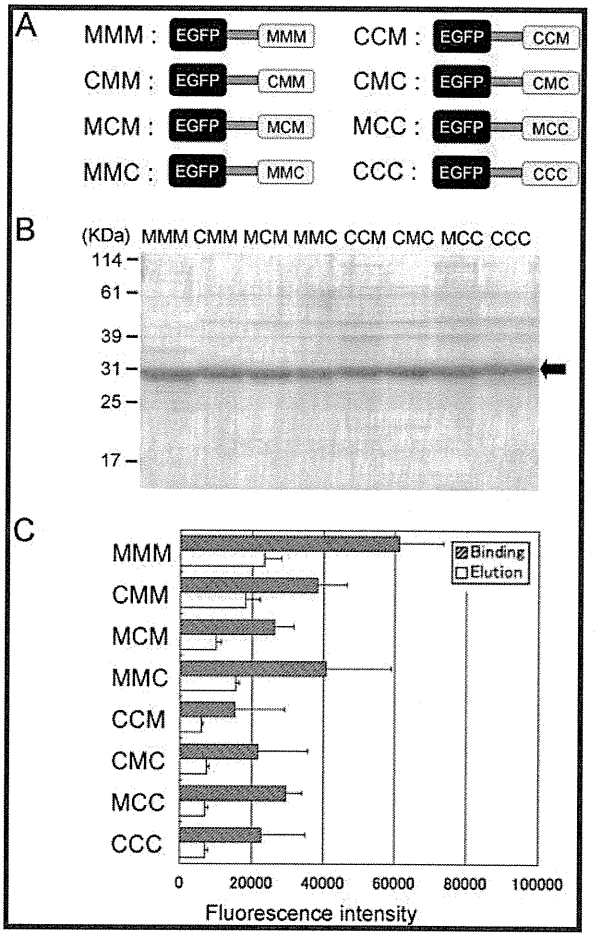

Figure 1. Binding affinity of tags comprising methionine and cysteine residues. (A) EGFPs tagged with peptides comprising three amino acids. The tags included methionine and/or cysteine and linked to the C-terminus of EGFP through a helix linker. (B) SDS-PAGE analysis of the tagged protein purified by ion exchange column chromatography. The gel was stained with Coomassie Brilliant Blue. The arrow indicates bands of tagged EGFPs. (C) Fluorescence intensities of the binding and eluted proteins obtained in the protein binding assay. The assay was performed three times. Each bar represents mean ± SD.

RESULTS

Three Amino Acid Tags Comprising Methionine and/or Cysteine. A goal of our research was to prepare a protein purification system using a novel peptide tag and GMP. To that end, we planned to develop novel peptide tags that specifically bind to GMP with high affinity. We first prepared eight peptide tags that included methionine and/or cysteine (MMM, CMM, MCM, MMC, CCM, CMC, MCC, and CCC), and each of them was fused to the C-terminus of EGFP with a polypeptide linker (Figure 1A and Supporting Information Figure S1). The tagged proteins were expressed in *E. coli* and purified with Q-Sepharose column chromatography (Figure 1B).

dx.doi.org/10.1021/bc100429d |*Bioconjugate Chem.* 2011, 22, 887–893

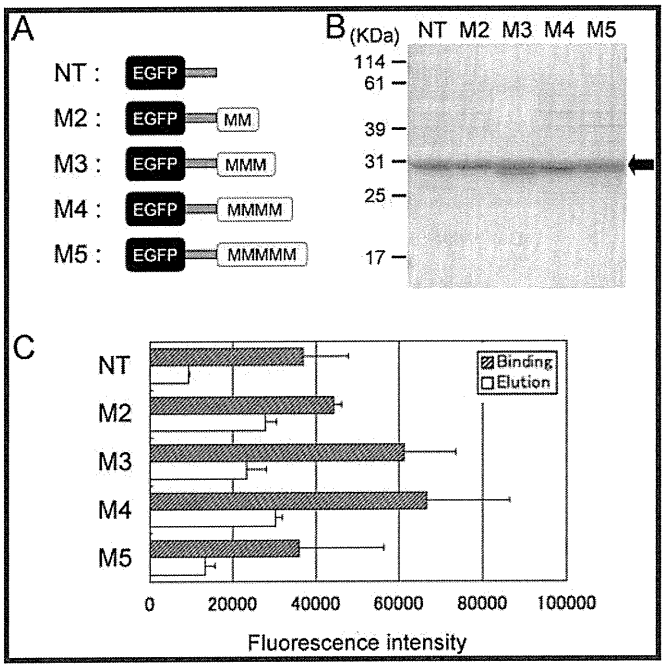

Figure 2. Binding affinity of tags comprising tandem methionine sequences. (A) EGFPs tagged with or without peptides comprising tandem methionine sequence. (B) SDS-PAGE analysis of the tagged protein purified by ion exchange column chromatography. The gel was stained with Coomassie Brilliant Blue. The arrow indicates bands of tagged EGFPs. (C) Fluorescence intensities of the binding and eluted proteins obtained in the protein binding assay. The assay was performed three times. Each bar represents mean ± SD.

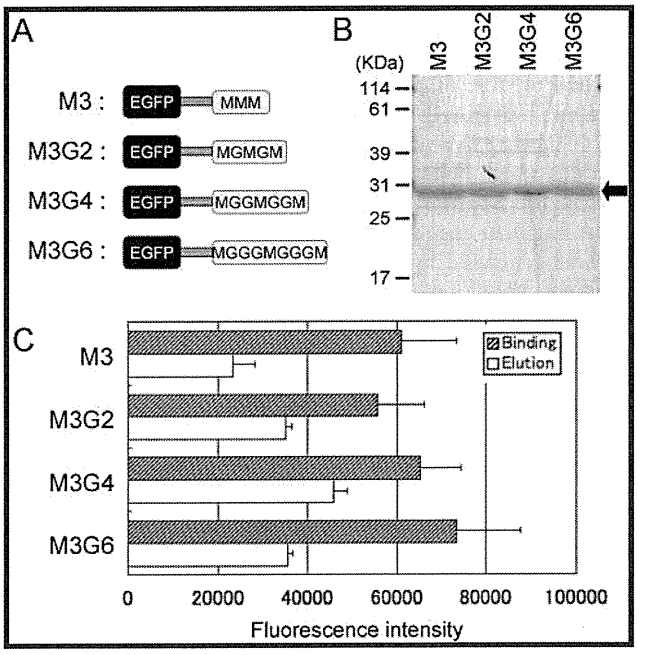

Figure 3. Binding affinity of the tags comprising methionine and glycine residues. (A) EGFPs tagged with the peptides comprising methionine and glycine residues. (B) SDS-PAGE analysis of the tagged protein purified by ion exchange column chromatography. The gel was stained with Coomassie Brilliant Blue. The arrow indicates bands of tagged EGFPs. (C) Fluorescence intensities of the binding and eluted proteins obtained in the protein binding assay. The assay was performed three times. Each bar represents mean ± SD.

A binding assay was performed to evaluate the affinity of the tagged proteins to GMP (Supporting Information Figure S4). Each of the tagged proteins was mixed with GMP for a binding reaction between GMP and the protein. The resulting GMP-protein complex was collected with a magnet and washed with the buffer to remove nonspecific binding proteins. The specific binding proteins were then eluted with the buffer containing 2-ME. Fluorescence intensities derived from binding and eluted protein were calculated by measuring the intensities of input, removed and eluted fractions (Figure 1D). MMM had the highest binding affinity for GMP. CMM and MMC had intermediate affinity for GMP (63% and 67% of the MMM intensity, respectively). MCM, CCM, CMC, MCC, CCC had low affinity for GMP (43%, 25%, 35%, 48%, and 37% of the MMM intensity, respectively). The fluorescence intensity of the eluted fraction showed the same pattern, that is, MMM had the highest intensity. CMM and MMC had intermediate affinity to GMP (78% and 66% of the MMM intensity, respectively). MCM, CCM, CMC, MCC, and CCC had low affinity to GMP (42%, 25%, 31%, 29%, and 29% of the MMM intensity, respectively). These results suggested that tags containing tandem methionine residues (e.g., MMM, CMM, and MMC) have high affinity to GMP.

Tandem Methionine Tags Containing Various Numbers of Methionine Residues. To further improve the binding affinity of the tandem methionine tag to GMP, we prepared tandem methionine tags comprising various numbers of methionine residues (M2, M4, and M5) and a control tag without methionine (NT) and coupled them to the C-terminus of EGFP (Figure 2A). These proteins were expressed in *E. coli* and purified with Q-Sepharose column chromatography (Figure 2B). Binding assays using these proteins showed that the fluorescence intensity of bound M3 and M4 was significantly higher than that of NT (1.7- and 1.8-fold compared to NT, respectively; Figure 2C). M2 had a moderately stronger intensity than NT (1.2-fold), while M5 and NT showed the similar intensities. A similar pattern was observed with the fluorescence intensities of the eluted proteins, with the exception of the strong intensity of M2 (the intensities of M2, M3, M4, and M5 were 3.0-, 2.6-, 3.3-, and 1.5-fold compared to NT). Together, these results indicate that the tags including three or four tandem methionine residues had the highest binding affinity to GMP and high elution efficiency from GMP.

Tags Comprising Three Methionine and Glycine Residues. To investigate whether the distance between methionine residues in the tag affects the binding affinity to GMP, 1 to 3 glycine residues (containing no sulfur atoms) were inserted between methionine residues of the M3 tag, and three new tags were prepared (Figure 3A). These tags were fused to the C-terminus of EGFP, and the tagged proteins (M3G2, M3G4, and M3G6) were expressed in *E. coli* and purified with Q-Sepharose column chromatography (Figure 3B). Binding assays using these proteins showed that the fluorescence intensity of binding proteins of M3G2, M3G4, and M3G6 were similar to that of M3 (0.9-, 1.1-, and 1.2-fold compared with M3, respectively; Figure 3C and Supporting Information Figure S5). In contrast, the fluorescence intensities of the eluted proteins containing M3G2, M3G4, and M3G6 were significantly higher than that of M3 (1.5-, 1.9-, and 1.5-fold compared to M3, respectively). This finding suggests that insertion of a glycine between methionine residues does not change the binding affinity of the tagged protein to GMP, and rather improved the elution efficiency.

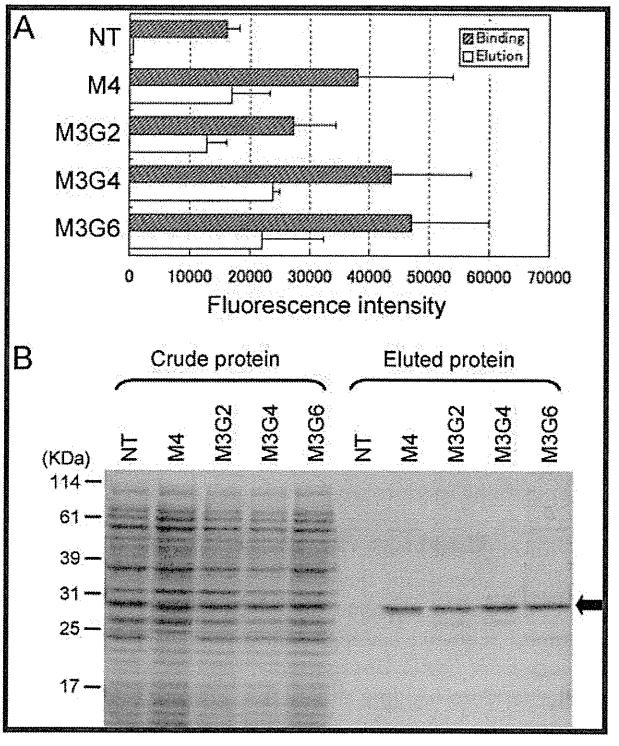

Figure 4. Purification of the tagged EGFPs from *E. coli* extract. (A) Fluorescence intensities of the binding and eluted proteins obtained in the protein purification assay. The assay was performed three times. Each bar represents mean ± SD. (B) SDS-PAGE analysis of the crude extract and purified protein. The arrow indicates bands of tagged EGFPs. The gel was stained with Coomassie Brilliant Blue.

Purification of the Tagged Protein from *E. coli* Extract. To investigate whether the tagged proteins can be purified from *E. coli* extract, each of five tagged or nontagged EGFPs (M4, M3G2, M3G4, M3G6, or NT) was expressed in *E. coli*. Crude protein extracts were prepared from *E. coli* and subjected to a protein purification assay. Fluorescence intensities of the binding proteins of M4, M3G2, M3G4, and M3G6 were significantly higher than that of NT (2.4-, 1.7-, 2.7-, and 2.9-fold, respectively; Figure 4A). Fluorescence intensities of the eluted proteins of M4, M3G2, M3G4, and M3G6 were also significantly higher than that of NT (51-, 38-, 72-, and 66-fold, respectively). These results indicate that tagged proteins were specifically purified by this purification step, though tag-independent nonspecific binding was observed with NT.

To further investigate the efficiency of the purification, the crude and eluted protein fractions were analyzed by SDS-PAGE following Coomassie Brilliant Blue staining (Figure 4B). The result indicated that the tagged EGFPs, but not the nontagged EGFP, were specifically purified from *E. coli* extract in very high purity. Together, these results indicated that the tagged proteins, including M4, M3G2, M3G4, and M3G6, can be purified from *E. coli* extract.

Improvement of the Purification Efficiency. A protein purification assay using tagged proteins indicated that there was tag-independent protein binding to GMP. To decrease this tag-independent protein binding to GMP, we treated GMP with phosphorylcholine (PC) and created GMP-PC. A binding assay using GMP or GMP-PC with NT showed that PC treatment resulted in a 65% decrease of the tag-independent protein

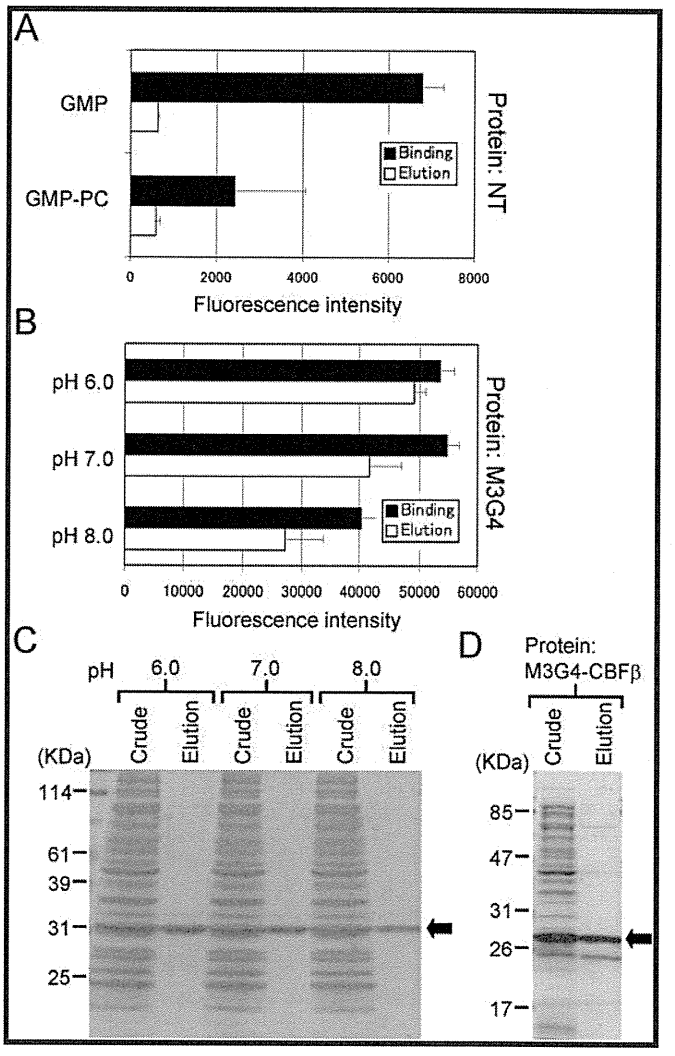

Figure 5. Treatment of GMP with phosphorylcholine improves the protein purification efficiency. (A) Fluorescence intensities of the binding and eluted proteins obtained in the protein purification assay using GMP or GMP-PC, and crude extract including NT. The assay was performed three times. Each bar represents mean ± SD. (B) Fluorescence intensities of the binding and eluted proteins obtained in the protein purification assay in pH 6–8 using GMP-PC and crude extract including M3G4. The assay was performed three times. Each bar represents mean ± SD. (C) SDS-PAGE analysis of the crude extract and purified protein. The arrow indicates bands of tagged EGFPs. The gel was stained with Coomassie Brilliant Blue. (D) Protein purification assay was performed using GMP-PC and *E. coli* extract containing M3G6 tagged CBFβ. The crude and eluted protein was analyzed by SDS-PAGE followed by Coomassie Brilliant Blue staining. The arrow indicates a band of tagged CBFβ.

binding to GMP, whereas the elution efficiency was not different between GMP and GMP-PC (Figure 5A). In addition, this PC treatment did not inhibit protein binding to GMP through gold nanoparticles (Supporting Information Figure S6). To determine the optimal pH for protein purification using GMP-PC, a protein purification assay was performed using M3G4 and buffers at pH 6, 7, and 8 (Figure 5B). The pH 6 and 7 buffers resulted in high fluorescence intensity of the binding proteins, while the pH 8 buffer resulted in 73% of intensity compared with the pH 6 and 7 buffers. In contrast, the fluorescence intensity of eluted protein was highest with the pH 6 buffer, while the pH 7

dx.doi.org/10.1021/bc100429d |*Bioconjugate Chem.* 2011, 22, 887–893

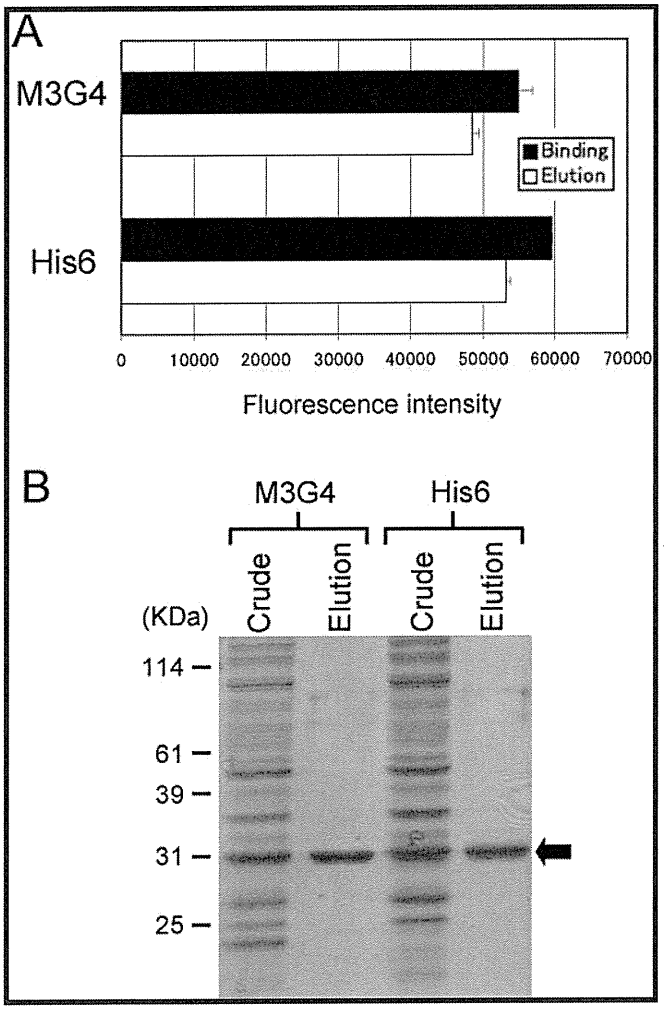

Figure 6. Comparison of the purification efficiency between system using a methionine tag or histidine tag. (A) Fluorescence intensities of the binding and eluted proteins obtained in the protein purification assay. The assay was performed three times. Each bar represents mean ± SD. (B) SDS-PAGE analysis of the crude extract and purified protein. The arrow indicates bands of tagged EGFPs. The gel was stained with Coomassie Brilliant Blue.

and 8 buffers showed reduced intensities (84% and 55% compared with pH 6, respectively). In this assay, 91%, 75%, and 67% of the binding proteins were eluted in pH 6, 7, and 8 buffers, respectively. To investigate the purity of the eluted protein, SDS-PAGE analysis was performed using crude and purified protein fractions (Figure 5C). The result showed that the tagged protein, M3G4, was specifically purified in all three buffers. In addition, another tagged protein, M3G4-CBFβ was also purified with GMP-PC in high purity (Figure 5D). Together, these results indicate that PC treatment of the GMP suppressed the tag-independent protein binding and significantly improved the efficiency of protein purification in buffer at a certain pH.

Comparison of Purification Efficiencies between Methionine Tag and Histidine Tag. To evaluate the efficiency of the established protein purification system in comparison with the common protein purification system, histidine-tagged EGFP (His6) was prepared. M3G4 or His6 was expressed in *E. coli*, and crude protein extracts were prepared. The same fluorescence intensity of the M3G4 and His6 was purified with the same amount (same iron weight) of GMP-PC or Co^{2+} chelated magnetic beads. Fluorescence intensities of both binding and eluted proteins of M3G4 were comparable to those of His6 (Figure 6A). SDS-PAGE analysis indicated that both M3G4 and His6 were specifically purified from the crude extract (Figure 6B). Together, these results indicate that the novel protein purification system using a methionine tag and GMP-PC has comparable efficiency to a common protein purification system.

DISCUSSION

We previously demonstrated that cystine (comprising 2 cysteine residues) and methionine specifically bind to GMP through Au—S binding and that cystine showed the significantly higher affinity to GMP than methionine.[23] On the basis of this finding, we hypothesized that peptide tags including methionine and/or cysteine residues would strongly bind to GMP. The aim of this study was to establish a novel protein purification system using novel peptide tags. To that end, we first generated the peptide tags comprising three amino acid peptide tags including methionine and/or cysteine residues. The tags with a tandem methionine sequence had high affinity to GMP and high elution efficiency from GMP. Unexpectedly, the tags with a number of cysteine residues had low affinity to GMP and also low elution efficiency, although cystine showed very strong affinity to GMP in our previous study.[23] We speculated that cysteine residues in the C-terminus of EGFP form intra- and/or intermolecular disulfide bonds, and that these might disturb the binding between the tags and GMP. In terms of the low elution efficiency of the tags with more than 2 cysteine residues, excessively strong binding between cysteine and GMP might inhibit the elution of the tagged EGFP.

The assay using three amino acid peptide tags indicated that tandem methionine residues improved the binding affinity of the tag. The binding assay using tandem methionine tags comprising different numbers of methionine residues indicated that increasing the number of methionine residues to four improved the binding affinity of the tag to GMP. However, the tag with five methionine residues has significantly decreased binding affinity to GMP. We speculated that the tag with five tandem methionine residues (M5) contributes to a hydrophobic interaction between tagged-EGFPs, which disturbs the Au—S binding between the tag and GMP. In addition, M5 expression level in *E. coli* was very low compared with that of M2, M3, or M4 (data not shown). A five tandem methionine sequence may disturb the protein expression in *E. coli*. This finding suggests that the tags with three or four methionine residues are preferable for protein purification.

We next hypothesized that the insertion of glycine residues between methionine residues would provide the peptide with a flexible conformation, thus making all the methionine residues contribute to Au—S binding, and we performed the assays using M3G2, M3G4, and M3G6. The insertion of glycine residues, however, did not change the binding affinity, but slightly improved the elution efficiency. Insertion of glycine residues might induce conformational changes of the tags and these tagged-EGFPs might then slightly increase the elution efficiency by improving the accessibility of 2-ME to the GMP.

The protein purification assays demonstrated that M4, M3G2, M3G4, and M3G6 can be purified from a protein mixture. However, not all the binding proteins were eluted from GMP, and this decreased the yield of the eluted protein. We speculated that this low purification efficiency derived from the nonspecific protein binding to GMP, which was observed in the binding assay

using NT. To decrease the nonspecific binding of protein to GMP, we treated GMP with PC that is known to have high free water fraction and decreased protein adsorption onto the polymer surface.[25−27] Treatment of GMP with PC and optimization of the buffer pH significantly reduced the nonspecific protein binding and increased the yield of the purified protein. Efficiency of the optimized protein purification system is comparable to that of the system using the histidine tag.

Thus, we successfully established a novel protein purification system using the novel peptide tags "methionine tags" and GMP. This purification system has several merits that are found in other protein purification systems. For example, the small tag sequence hardly interferes with protein expression in cells and does not affect protein structure and functions. Specialized binding buffers and substrates for protein elution are not necessary. All of the purification steps can be easily and quickly performed by using a magnet instead of a centrifuge. Thus, this protein purification system is convenient and useful. In addition, GMPs conjugated with methionine-tagged protein might be useful as tools for biological and clinical research.

■ ASSOCIATED CONTENT

Supporting Information. Information regarding the polypeptide linker sequence (Figure S1), construction of plasmids (Figure S2 and S3), protein purification procedure (Figure S4), protein binding assay using various amounts of proteins (Figure S5), and protein purification assay using magnetic particles (Figure S6). This material is available free of charge via the Internet at http://pubs.acs.org.

■ AUTHOR INFORMATION

Corresponding Author

*Yoshiaki Okada, Ph.D., Osaka University, Graduate School of Pharmaceutical Sciences, 1-6 Yamadaoka, Suita, Osaka, 565-0871, Japan. E-mail: okadabos@phs.osaka-u.ac.jp. Tel/Fax: +81-6-6879-8164.

Author Contributions

#Y.O. and T.Y.T. equally contributed to this work.

■ ACKNOWLEDGMENT

This work was supported by the Japan Science and TechnologyAgency (JST).

■ REFERENCES

(1) Schmidt, T. G., and Skerra, A. (1993)The random peptide library-assisted engineering of a C-terminal affinity peptide, useful for the detection and purification of a functional Ig Fv fragment. *Protein Eng. 6*, 109–22.

(2) di Guan, C., Li, P., Riggs, P. D., and Inouye, H. (1988)Vectors that facilitate the expression and purification of foreign peptides in Escherichia coli by fusion to maltose-binding protein. *Gene 67*, 21–30.

(3) Kapust, R. B., and Waugh, D. S. (1999)Escherichia coli maltose-binding protein is uncommonly effective at promoting the solubility of polypeptides to which it is fused. *Protein Sci. 8*, 1668–74.

(4) Einhauer, A., and Jungbauer, A. (2001)The FLAG peptide, a versatile fusion tag for the purification of recombinant proteins. *J. Biochem. Biophys. Methods 49*, 455–65.

(5) Gaberc-Porekar, V., and Menart, V. (2001)Perspectives of immobilized-metal affinity chromatography. *J. Biochem. Biophys. Methods 49*, 335–60.

(6) Marti, D., Schaller, J., Ochensberger, B., and Rickli, E. E. (1994) Expression, purification and characterization of the recombinant kringle 2 and kringle 3 domains of human plasminogen and analysis of their binding affinity for omega-aminocarboxylic acids. *Eur. J. Biochem. 219*, 455–62.

(7) Vaillancourt, P., Zheng, C. F., Hoang, D. Q., and Breister, L. (2000)Affinity purification of recombinant proteins fused to calmodulin or to calmodulin-binding peptides. *Methods Enzymol. 326*, 340–62.

(8) Schatz, P. J. (1993)Use of peptide libraries to map the substrate specificity of a peptide-modifying enzyme: a 13 residue consensus peptide specifies biotinylation in Escherichia coli. *Bio/Technology 11*, 1138–43.

(9) Voss, S., and Skerra, A. (1997)Mutagenesis of a flexible loop in streptavidin leads to higher affinity for the Strep-tag II peptide and improved performance in recombinant protein purification. *Protein Eng. 10*, 975–82.

(10) Kamei, K., Mukai, Y., Kojima, H., Yoshikawa, T., Yoshikawa, M., Kiyohara, G., Yamamoto, T. A., Yoshioka, Y., Okada, N., Seino, S., and Nakagawa, S. (2009)Direct cell entry of gold/iron-oxide magnetic nanoparticles in adenovirus mediated gene delivery. *Biomaterials 30*, 1809–14.

(11) Konishi, Y., Lindholm, K., Yang, L. B., Li, R., and Shen, Y. (2002) Isolation of living neurons from human elderly brains using the immunomagnetic sorting DNA-linker system. *Am. J. Pathol. 161*, 1567–76.

(12) Hoshino, A., Ohnishi, N., Yasuhara, M., Yamamoto, K., and Kondo, A. (2007)Separation of murine neutrophils and macrophages by thermoresponsive magnetic nanoparticles. *Biotechnol. Prog. 23*, 1513–6.

(13) Vonderheide, R. H., and June, C. H. (2003)A translational bridge to cancer immunotherapy: exploiting costimulation and target antigens for active and passive T cell immunotherapy. *Immunol. Res. 27*, 341–56.

(14) Lemke, A. J., Senfft von Pilsach, M. I., Lubbe, A., Bergemann, C., Riess, H., and Felix, R. (2004)MRI after magnetic drug targeting in patients with advanced solid malignant tumors. *Eur. Radiol. 14*, 1949–55.

(15) Fortin-Ripoche, J. P., Martina, M. S., Gazeau, F., Menager, C., Wilhelm, C., Bacri, J. C., Lesieur, S., and Clement, O. (2006)Magnetic targeting of magnetoliposomes to solid tumors with MR imaging monitoring in mice: feasibility. *Radiology 239*, 415–24.

(16) Ito, A., Shinkai, M., Honda, H., and Kobayashi, T. (2001)Heat-inducible TNF-alpha gene therapy combined with hyperthermia using magnetic nanoparticles as a novel tumor-targeted therapy. *Cancer Gene Ther. 8*, 649–54.

(17) Ito, A., Shinkai, M., Honda, H., and Kobayashi, T. (2005) Medical application of functionalized magnetic nanoparticles. *J. Biosci. Bioeng. 100*, 1–11.

(18) Gabrielsen, O. S., Hornes, E., Korsnes, L., Ruet, A., and Oyen, T. B. (1989)Magnetic DNA affinity purification of yeast transcription factor tau--a new purification principle for the ultrarapid isolation of near homogeneous factor. *Nucleic Acids Res. 17*, 6253–67.

(19) Seino, S., Kinoshita, T., Otome, Y., Okitsu, K., Nakagawa, T., and Yamamoto, T. A. (2003)Magnetic composite nanoparticles of Au/gamma-Fe_2O_3 synthesized by gammma-ray irradiation. *Chem. Lett. 32*, 690–691.

(20) Kinoshita, T., Seino, S., Okitsu, K., Nakayama, T., Nakagawa, T., and Yamamoto, T. A. (2003)Magnetic evaluation of nanostructure of gold-iron composite particles synthesized by a reverse micelle method. *J. Alloys Compd. 359*, 46–50.

(21) Nuzzo, R. G., and Allara, D. L. (1983)Adsorption of bifunctional organic disulfides on gold surfaces. *J. Am. Chem. Soc. 105*, 4481–4483.

(22) Karyakin, A. A., Presnova, G. V., Rubtsova, M. Y., and Egorov, A. M. (2000)Oriented immobilization of antibodies onto the gold surfaces via their native thiol groups. *Anal. Chem. 72*, 3805–3811.

(23) Kinoshita, T., Seino, S., Mizukoshi, Y., Otome, Y., Nakagawa, T., Okitsu, K., and Yamamoto, T. A. (2005)Magnetic separation of amino acids by gold/iron-oxide composite nanoparticles synthesized by gamma-ray irradiation. *J. Magn. Magn. Mater. 293*, 106–110.

(24) Seino, S., Kinoshita, T., Nakagawa, T., Kojima, T., Taniguci, R., Okuda, S., and Yamamoto, T. A. (2008)Radiation induced synthesis of gold/iron-oxide composite nanoparticles using high-energy electron beam. *J. Nanopart. Res. 10*, 1071–1076.

(25) Ishihara, K., Ishikawa, E., Iwasaki, Y., and Nakabayashi, N. (1999)Inhibition of fibroblast cell adhesion on substrate by coating with 2-methacryloxloxyethyl phosphorylcholine polymers. *J. Biomater. Sci., Polym. Ed. 10*, 1047–1061.

(26) Lu, D. R., Lee, S. J., and Park, K. (1991) Calculation of solvation interaction energies for protein adsorption on polymer surfaces. *Journal of biomaterials science. Polymer edition 3*, 127—147.

(27) Maeno, K., Hirayama, A., Sakuma, K., and Miyazawa, K. (2011) An activated medium with high durability and low nonspecific adsorption: Application to protein A chromatography. *Anal. Biochem. 409*, 123–129.

blood

2011 117: 342-351
Prepublished online October 27, 2010;
doi:10.1182/blood-2010-06-287987

Vascular bed–specific regulation of the von Willebrand factor promoter in the heart and skeletal muscle

Ju Liu, Lei Yuan, Grietje Molema, Erzsébet Regan, Lauren Janes, David Beeler, Katherine C. Spokes, Yoshiaki Okada, Takashi Minami, Peter Oettgen and William C. Aird

Blood (print ISSN 0006-4971, online ISSN 1528-0020), is published weekly by the American Society of Hematology, 2021 L St, NW, Suite 900, Washington DC 20036.

Vascular bed–specific regulation of the von Willebrand factor promoter in the heart and skeletal muscle

Ju Liu,[1,2] Lei Yuan,[1,2] Grietje Molema,[1,3] Erzsébet Regan,[1,2] Lauren Janes,[1,2] David Beeler,[1,2] Katherine C. Spokes,[1,2] Yoshiaki Okada,[4] Takashi Minami,[5] Peter Oettgen,[1,2] and William C. Aird[1,2]

[1]Center for Vascular Biology Research and Division of Molecular and Vascular Medicine, Beth Israel Deaconess Medical Center, Boston, MA; [2]Division of Molecular and Vascular Medicine, Department of Medicine, Beth Israel Deaconess Medical Center, Boston, MA; [3]Department of Pathology and Medical Biology, University Medical Center Groningen, University of Groningen, Groningen, The Netherlands; [4]Graduate School of Pharmaceutical Sciences, Osaka University, Osaka, Japan; and [5]Research Center for Advanced Science and Technology, University of Tokyo, Tokyo, Japan

A region of the human von Willebrand factor (*VWF*) gene between −2812 and the end of the first intron (termed vWF2) was previously shown to direct expression in the endothelium of capillaries and a subset of larger blood vessels in the heart and skeletal muscle. Here, our goal was to delineate the DNA sequences responsible for this effect. A series of constructs containing deletions or mutations of vWF2 coupled to LacZ were targeted to the *Hprt* locus of mice, and the resulting animals were analyzed for reporter gene expression. The findings demonstrate that DNA sequences between −843 and −620 are necessary for expression in capillary but not large vessel endothelium in heart and skeletal muscle. Further, expression of VWF in capillaries and larger vessels of both tissues required the presence of a native or heterologous intron. In vitro assays implicated a role for ERG-binding ETS motif at −56 in mediating basal expression of VWF. In *Hprt*-targeted mice, mutation of the ETS consensus motif resulted in loss of LacZ expression in the endothelium of the heart and skeletal muscle. Together, these data indicate that distinct DNA modules regulate vascular bed–specific expression of VWF. (*Blood.* 2011;117(1):342-351)

Introduction

The von Willebrand factor (VWF) is a high-molecular weight glycoprotein that mediates platelet-vessel wall interactions. VWF is expressed specifically in endothelial cells and megakaryocytes. Its expression in the intact endothelium varies both spatially and temporally. For example, in mice VWF mRNA levels are higher in the lung and heart compared with the liver and kidney, and within a given tissue, VWF expression is generally greater on the venous side of the circulation.[1] Expression of VWF may change in pathophysiological conditions. For example, in a mouse model of endotoxemia, VWF mRNA levels were down-regulated in aorta, brain, adipose tissue, testis, thymus, adrenal, skeletal muscle, gut, and liver but increased in the heart and kidney.[1] The elucidation of the mechanisms underlying VWF expression may provide important insights into the molecular basis of vascular diversity.

The structural organization of the mouse, human, and bovine VWF promoter-proximal region is closely related.[2-4] The first exon (+1 to +246 in human VWF) encodes 5′ untranslated sequence. The second exon contains the ATG translational start site. Exons 1 and 2 are separated by an intron (+247 to +1475 in human VWF). A previous in vitro analysis of the human gene demonstrated that a 734-bp region between −487 and +246 contains information for lineage-specific expression in cultured endothelial cells.[5] In standard transgenic mice, this promoter fragment (which we have termed vWF1) retained endothelial cell specificity. However, expression was limited to blood vessels of the brain.[6] In contrast, standard transgenic mice carrying a larger region of the *VWF* gene (between −2182 and the end of the first intron; designated vWF2) directed expression not only in blood vessels of the brain but also in capillaries of the heart and skeletal muscle.[7] A similar fragment from the mouse VWF promoter displayed an identical pattern of expression, supporting interspecies similarities in transcriptional control mechanisms.[2]

To control for copy number and integration site, we targeted a single copy of the vWF2-LacZ cassette to the *Hprt* locus of mice. Consistent with the results of the standard transgenic mice, the *Hprt*-targeted vWF2 promoter directed expression in the vasculature of the brain, heart, and skeletal muscle but not in other organs such as aorta, lung, liver, spleen, and kidney.[8]

The goal of this study was to further delineate the DNA sequences involved in mediating vascular bed–specific expression of the *VWF* gene. We report that a 224-bp region between −843 and −620 in the upstream promoter is necessary for expression in the capillaries of the heart and skeletal muscle. These DNA sequences are distinct from those that regulate expression in venous endothelium in these 2 organs. Furthermore, we demonstrate that promoter activity in the capillaries and certain larger vessels of the heart and skeletal muscle requires a native or heterologous intron as well as an intact ERG-binding site at −56. These data support a model of gene regulation whereby a constellation of vascular bed–specific DNA regions or modules govern overall expression of VWF in the endothelium. Further, the results underscore the importance of studying gene regulation in the context of the intact endothelium.

Submitted May 29, 2010; accepted August 31, 2010. Prepublished online as *Blood* First Edition paper, October 27, 2010; DOI 10.1182/blood-2010-06-287987.

The online version of this article contains a data supplement.

The publication costs of this article were defrayed in part by page charge payment. Therefore, and solely to indicate this fact, this article is hereby marked "advertisement" in accordance with 18 USC section 1734.

Methods

Plasmid constructions

Construction of VWF deletion and mutant promoter constructs used in transient transfection assays and *Hprt*-locus targeting is detailed in supplemental Methods (available on the *Blood* Web site; see the Supplemental Materials link at the top of the online article). The constructs are schematically shown in Figure 1.

Cell culture and transfections

Human umbilical vein endothelial cells (HUVECs) were purchased from Lonza and cultured in endothelial cell medium supplemented with microvascular endothelial cell growth medium-2 (bullet kit; Lonza).

Transient transfection assays

Transient transfections were carried out as described in supplemental Methods.

ChIP assay

Chromatin immunoprecipitation (ChIP) assays were performed using a ChIP assay kit (Upstate Biotechnology Inc.) according to the manufacturer's instructions and as detailed in supplemental Methods.

Transfection with siRNA

HUVECs were transfected with siRNA against ERG as previously described.[9]

Quantitative reverse transcriptase PCR

Quantitative reverse transcriptase polymerase chain reaction (PCR) was carried out as previously described.[9,10]

Generation and analysis of *Hprt*-targeted transgenic mice

The generation of *Hprt*-vWF2-LacZ mice was previously described.[8] All animal experiments were approved by the Beth Israel Deaconess Medical Center Institutional Animal Care and Use Committee. To generate the additional *Hprt*-targeted mice, the targeting vectors were linearized with *Sal*I and transfected into BK4-embryonic stem cells by electroporation. Homologous recombinants were selected in HAT (hypoxanthine-aminopterin-thymidine)–supplemented medium, containing 0.1mM hypoxanthine, 0.0004mM aminopterin, and 0.016mM thymidine (Sigma-Aldrich). HAT-resistant colonies were picked 10 days later for propagation, and a subset of the cells were examined for homologous recombination by LacZ PCR. Targeted embryonic stem cells were injected into C57BL/6-derived blastocysts that were then transplanted into the uteri of recipient Swiss Webster females. Resulting chimeric males were bred with C57BL/6 females to obtain agouti offspring. The agouti female offspring were backcrossed with C57BL/6 males to generate hemizygous male F2 mice. Genotyping was performed by PCR analysis. Whole-mount LacZ staining in adult male tissues was carried out as previously described.[6] Smooth muscle actin staining was carried out as described in supplemental Methods.

Bioinformatics

Development and analysis of DNA microarray compendiums and analysis of the human, mouse, and bovine VWF promoters are described in supplemental Methods.

Statistical analysis

Data are expressed as mean ± SE or SD. The statistical significance of differences of the means was determined by 1-way analysis of variance and multiple comparisons by Tukey-Kramer multiple range test.

Results

DNA sequences between −2182 and −487 and/or in the first intron (between +247 and +1475) contain information for expression in vascular beds of the heart and skeletal muscle

Previous studies in standard transgenic mice demonstrated that the vWF1 promoter (between −487 and +246) directed expression in blood vessels of the brain,[6] whereas the larger vWF2 promoter fragment (between −2182 and +1475) directed expression not only in the vascular endothelium of the brain but also in the capillary endothelium of the heart and skeletal muscle.[7] When targeted as a single-copy transgene to the *Hprt* locus of mice, vWF2-lacZ demonstrated an identical expression pattern to that of the standard transgenic mice with the exception that it was also active in a subset of larger vessels of the heart and skeletal muscle (supplemental Figure 1).[8] In tissue sections of the heart, these larger vessels comprised veins and venules, as defined by their wide diameter and thin wall and low reactivity to antismooth muscle actin antibody (supplemental Figures 2-3). In tissue sections of the diaphragm, the majority of staining in noncapillary endothelial cells also occurred in veins and venules. However, in contrast to the heart, the diaphragm revealed occasional LacZ-positive endothelial cells in arterioles (supplemental Figure 4). LacZ expression was not detected in other organs examined, including the aorta, liver, spleen, lung, and kidney (supplemental Figure 5).

We extended our findings by targeting vWF1 to the *Hprt* locus. As in standard transgenic mice, vWF1 promoter activity was limited to blood vessels of the brain (supplemental Figure 1). Although the pattern of LacZ expression in the brain was similar between vWF1 and vWF2 lines, overall promoter activity was lower in vWF1 mice. Thus, information for expression in the vascular endothelium of the heart and skeletal muscle is contained within DNA sequences between −487 and −2182 and/or in the first intron (between +247 and +1475).

A region between −843 and −620 contains information for expression in the capillary endothelium of the heart and skeletal muscle

To further delineate the promoter regions responsible for expression in blood vessels of the heart and skeletal muscle, we targeted a series of deletion constructs to the *Hprt* locus of mice (Figure1). 5′-deletion variants of vWF2 containing 1143-bp 5′-flanking sequence (vWF2-Del1-lacZ) and 843-bp 5′-flanking sequence (vWF2-Del2-lacZ) retained promoter activity in the endothelium of capillaries and larger vessels in the heart and skeletal muscle, while 5′-deletion constructs containing 620 bp (vWF2-Del3-lacZ) or 487 bp (vWF2-Del4-lacZ) were expressed in a similar subset of macrovessels but not in capillaries of the heart and skeletal muscle (Figure 2 and supplemental Figures 6-7).

Based on the results of the 5′-deletion analysis, we generated a vWF2 promoter-LacZ cassette containing an internal deletion of DNA sequences between −843 and −620. When targeted to the *Hprt* locus of mice, the resulting construct (vWF2-$\Delta_{843\text{-}620}$-lacZ) also demonstrated an identical expression pattern to that of vWF2-Del3-lacZ, with selective loss of capillary expression in the heart and skeletal muscle (Figures 2-3 and supplemental Figures 5-9). Together, these data indicate that a region between −843 and −620 contains information for expression of VWF in the capillary endothelium of the heart and skeletal muscle, whereas a region

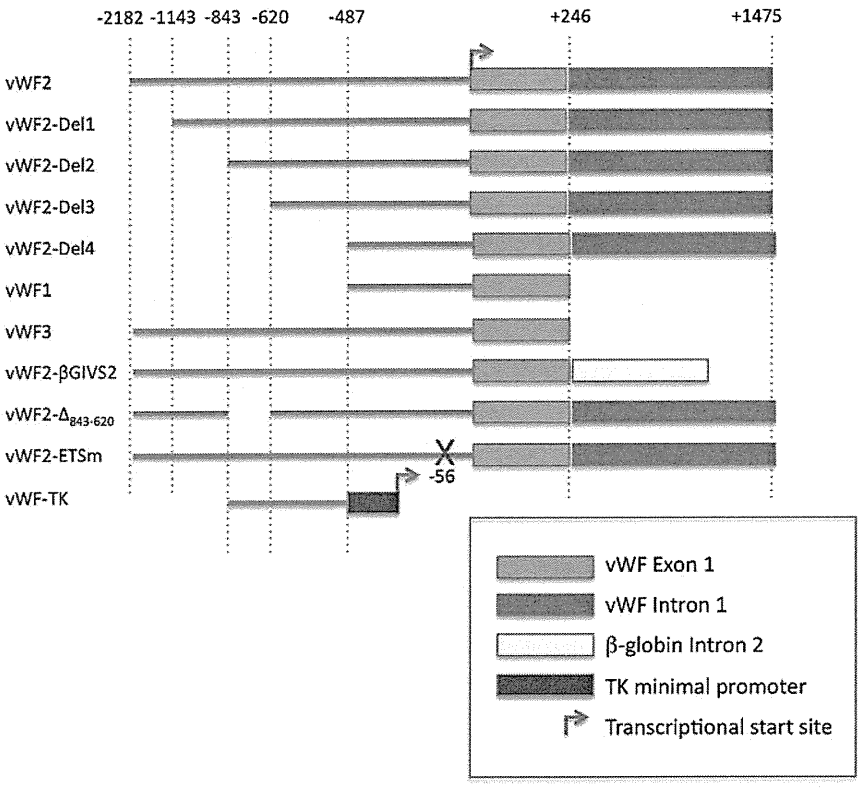

Figure 1. Schematic of the human VWF promoter fragments used in transfections and *Hprt*-targeted mice. TK, thymidine kinase.

between −620 and +1475 confers expression in the veins/venules of the heart and veins/venules and occasional arterioles of skeletal muscle.

Intronic splicing is necessary for expression in the capillary endothelium of the heart and skeletal muscle

Previous studies have demonstrated a role for intronic enhancers in mediating the expression of other endothelial cell-specific promoters in vivo, including vascular endothelial growth factor receptor 2/fetal liver kinase (FLK)1, TIE-2, GATA2, and endoglin.[11-15] Thus, we asked whether the first intron of VWF plays a role in mediating vascular bed–specific expression of the gene. To that end, we generated *Hprt*-targeted mice with an intron-less version of vWF2 (between −2182 and +246; termed vWF3) coupled to LacZ. Similar to vWF1 (-487 to +246), vWF3 promoter activity was limited to blood vessels of the brain (Figure 4). These findings suggested that the first intron of VWF plays an important role in mediating VWF expression in the heart and skeletal muscle.

Other studies using standard transgenic mice have shown that intronic splicing per se may result in increased expression of the transgene in nonendothelial cells.[16-19] To test the possibility that such a mechanism is involved in mediating VWF expression, we replaced the first intron of VWF with the second intron (intervening sequence 2 [IVS2]) of the human β-globin gene. We chose this particular intron because it has been shown to increase the expression of native and heterologous transgenic promoters by an enhancer-independent mechanism.[16,20] The resulting *Hprt*-targeted mice (termed vWF2-βGIVS2-lacZ) revealed an identical pattern of expression to that of vWF2-lacZ mice (Figure 4 and supplemental Figure 10). These findings suggest that VWF promoter activity in the heart and skeletal muscle is dependent on intronic splicing. The absolute level of vWF2-βGIVS2-lacZ expression was, however, lower compared with vWF2-lacZ. Thus, the native intron of VWF may also contain positive-acting DNA elements.

To determine whether the microvascular and/or macrovascular-specific region of the VWF promoter functions as an autonomous enhancer, a fragment spanning the region between −843 and −487 was coupled to the 5′ end of the thymidine kinase (TK) promoter and LacZ, and the resulting construct (VWF enhancer-TK-lacZ) was targeted to the *Hprt* locus. TK-lacZ demonstrated high-level expression in cardiomyocytes but not in skeletal muscle. The addition VWF promoter sequences between −843 and −620 did not affect the level or pattern of expression (supplemental Figure 11 shows diaphragm). Thus, this DNA region does not function as an autologous enhancer.

An ERG-binding motif at −56 is necessary for vWF2 promoter activity in vivo

We recently reported that a mutation of a GATA motif at +220 in vWF2 results in moderately reduced promoter activity in the heart, skeletal muscle, and brain of *Hprt*-targeted mice.[10] Thus, it is likely that vascular bed–specific regions of the promoter (such as the one between −843 to −620) require proximal promoter elements for basal activity in their respective vascular beds. To further test this hypothesis, we focused on an ETS motif (TTCC) at −56. A previous study showed that this site binds the ETS factor ERG but not ETS-1/2 and that it positively regulates VWF promoter activity.[21] Bioinformatic approaches offer additional insights into the potential role of the −56 ETS site and the ERG transcription factor in regulating VWF expression. For example, cross-species sequence comparisons of the proximal VWF promoter reveal evolutionary conservation of the −56 ETS motif (supplemental Figure 12). As a second strategy, we plotted expression levels of ERG and VWF across 2 compendia of publicly available DNA microarray experiments. The first such compendium is dominated by endothelial cells and smooth muscle cells of heterogeneous origin. It includes transcriptional profiles from 53 purified endothelial cell samples, representing 14 distinct locations, all propagated

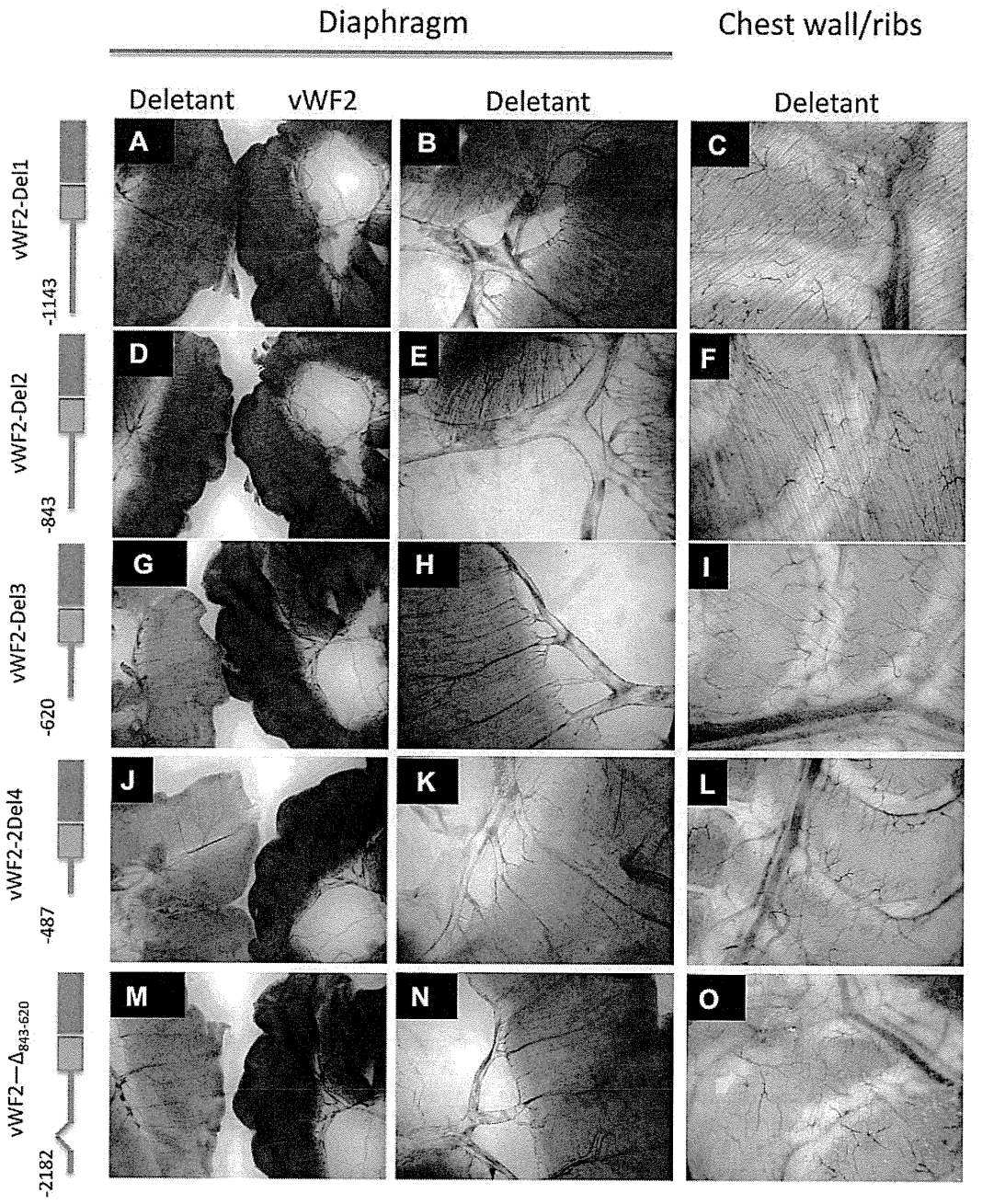

Figure 2. LacZ staining of diaphragm and chest wall from *Hprt*-targeted mice carrying vWF2-lacZ or deletant VWF promoter-lacZ constructs. Diaphragms and chest walls were harvested from 6- to 8-week-old F2 male *Hprt*-targeted mice carrying vWF2-lacZ or deletant VWF transgenes and processed in parallel for whole-mount staining with X-Gal. In the left-most column (A,D,G,J,M), the diaphragm from the vWF2-lacZ transgenic mouse is on the right, and the diaphragm from the deletant VWF transgenic mouse is on the left. Panels in the second column (B,E,H,K,N) represent higher power images of the deletant VWF transgenic tissues shown A, D, G, J, and M, respectively. Wild-type vWF2-lacZ and all 5 deletant VWF transgenic mice demonstrate LacZ staining in macrovessels of skeletal muscle (diaphragm and intercostal muscle). However, note the loss of microvascular LacZ staining in vWF2-Del3-lacZ, vWF2-Del4-lacZ, and vWF2-$\Delta_{843\text{-}620}$-lacZ tissues. Whole-mount tissues were analyzed under a Nikon SMZ-U dissecting microscope, and microphotographs were collected using a Nikon Coolpix 8400 camera.

in identical culture conditions.[22] The sample set included endothelial cells from 5 different arteries (aorta, coronary artery, pulmonary artery, iliac artery, and umbilical artery), 2 different veins (umbilical vein and saphenous vein), and 7 different tissues (skin, lung, intestine, uterus myometrium, nasal polyps, bladder, and myocardium).[22] These arrays are complemented by 60 profiles of smooth muscle cells representing a similar set of locations and a study of hypoxia and serum starvation of endothelial cells, smooth muscle cells, and 2 lines of epithelial cells (64 further arrays).[23,24] We assembled a second compendium of 5532 microarray experiments restricted to human cells, as described in supplemental Methods. As shown in Figure 5A, the correlation between VWF and ERG transcription factor mRNA levels was very high within the endothelial cell population, as well as within all arrays of the compendium representing multiple cell types and tissue samples. Indeed, ERG ranked second among 1081 genes that are annotated by GO with "transcriptional regulatory activity" based on correlation and ranked fourth based on mutual information. Although there is no guarantee that transcription factor mRNA levels reflect their transcriptional activity, these unbiased data strongly suggest that ERG plays an important role in mediating VWF expression.

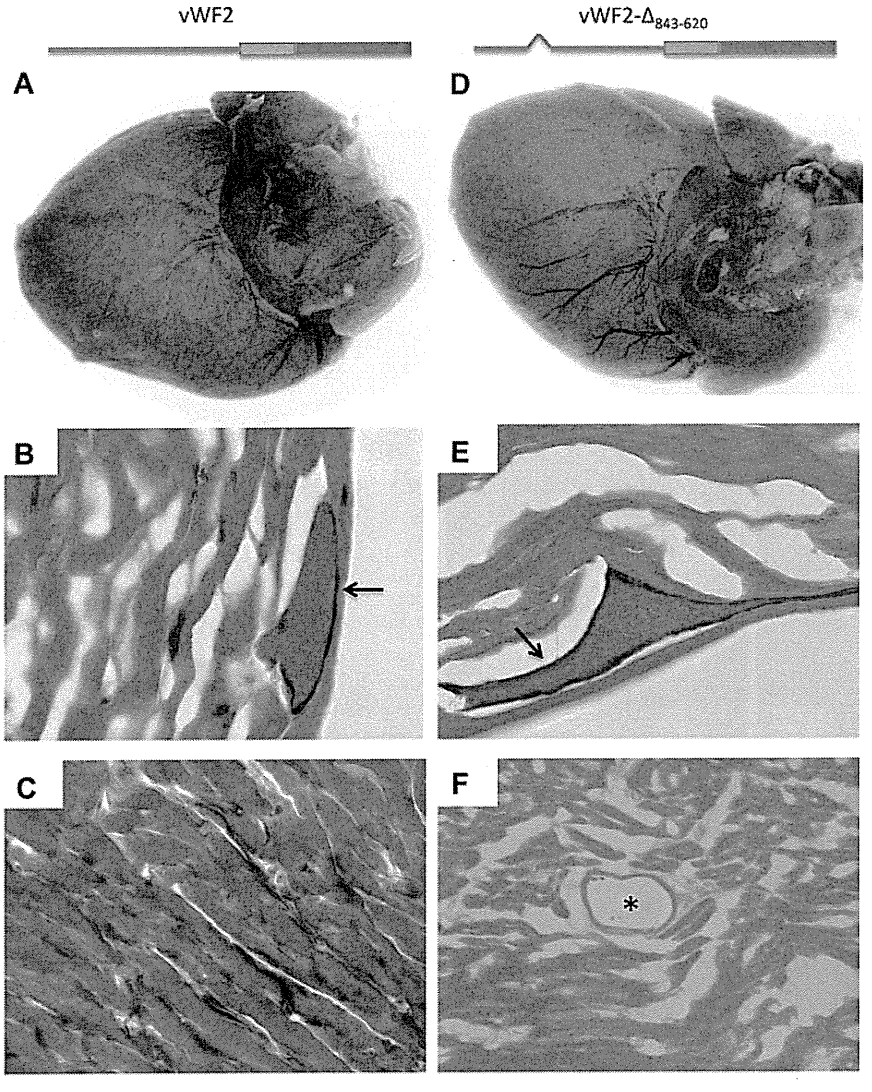

Figure 3. LacZ staining of heart whole mounts and tissue sections from vWF2-lacZ and vWF2-$\Delta_{843-620}$-lacZ mice. Hearts were harvested from 6- to 8-week-old F2 male *Hprt*-targeted mice carrying vWF2-lacZ transgene (A-C) or vWF2-$\Delta_{843-620}$-lacZ transgene (identical to vWF2 except for an internal deletion of DNA sequences between −843 and −620; D-F) and processed in parallel for whole-mount (A,D) or cryosection (B-C,E-F) staining with X-Gal. vWF2-lacZ and vWF2-$\Delta_{843-620}$-lacZ transgenic hearts demonstrate LacZ staining in veins. However, note loss of capillary endothelial staining in the vWF2-$\Delta_{843-620}$-lacZ heart. Whole-mount hearts were analyzed under a Nikon SMZ-U dissecting microscope, and microphotographs were collected using a Nikon Coolpix 8400 camera. Tissue section images were obtained using a ×100 objective (B,E), ×60 objective (C), or ×40 objective (F). Lac-Z-stained sections were counterstained with eosin. Slides were analyzed under a Zeiss Axio Imager upright microscope, and photomicrographs were collected using a Zeiss Axiocam MRc camera and Axiovision 4.6.3 image acquisition software. Arrow, LacZ staining in venous endothelial cells. Asterisk, lumen of an artery.

A previous study showed that ERG knockdown in HUVECs or incubation of HUVECs with tumor necrosis factor-α (TNF-α) reduced the expression of several endothelial genes, including *VWF*.[25] We recently demonstrated that TNF-α suppresses ERG expression in endothelial cells.[9] To confirm that TNF-α results in concomitant inhibition of ERG and VWF, HUVECs were treated with 20 ng/mL TNF-α for varying times and assayed for mRNA expression using quantitative real-time PCR. As shown in Figure 5B, TNF-α resulted in a time-dependent reduction in ERG and VWF mRNA (46% and 52% of control at 24 hours, respectively) but not CD31, β-actin, or the ETS transcription factor, friend leukemia virus integration (Fli)–1. To assay for ERG binding to the proximal VWF promoter, we performed ChIP assays in HUVECs treated in the absence or presence of 20 ng/mL TNF-α for 12 hours. Native chromatin was immunoprecipitated with antibodies against ERG or control IgG, and the immunoprecipitated fractions were subjected to PCR using VWF exon 1-specific primers. As shown in Figure 5C, the immediate upstream promoter of VWF (which contains the −56 ETS motif) was bound by ERG, and the level of binding was significantly reduced by TNF-α treatment. In transient transfection assays of HUVECs, a mutation of the −56 ETS site (from GGAA to TTAA) resulted in a slight but significant reduction (72.2% of untreated vWF2 control) in basal promoter activity (Figure 5D). TNF-α treatment of transfected HUVECs inhibited the activity of vWF2 (74.4% of untreated vWF2 control) but not vWF2-ETSm (Figure 5D).

To further verify a functional role for ERG binding to the −56 ETS site in mediating VWF promoter activity, we used siRNA against ERG to knock down ERG expression in HUVECs and transfected these cells with wild-type (vWF2) or mutant VWF promoter-reporter gene constructs. ERG knockdown resulted in significant inhibition of ERG mRNA (18% of control) and VWF mRNA (37% of control), as assayed by quantitative real-time PCR (Figure 5E). siRNA-mediated down-regulation of ERG protein was confirmed in Western blot analyses (Figure 5F). In ERG-deficient cells, vWF2 promoter activity was reduced to 45% of control (CTR siRNA) levels (Figure 5G). Consistent with the data shown in Figure 5D, vWF2-ETSm demonstrated lower activity in untreated or control siRNA-treated HUVECs, implicating a functional role for the −56 ETS motif (Figure 5G). vWF2 and vWF2-ETSm demonstrated comparable activity in knockdown cells, suggesting that ERG mediates vWF2 expression via the −56 ETS site (Figure 5G). There was a further small reduction in vWF2-ETSm activity in ERG-deficient cells compared with control cells. Together, these in vitro data strongly suggest that ERG binds to the −56 ETS site and that the resulting DNA-protein interaction positively regulates VWF expression.

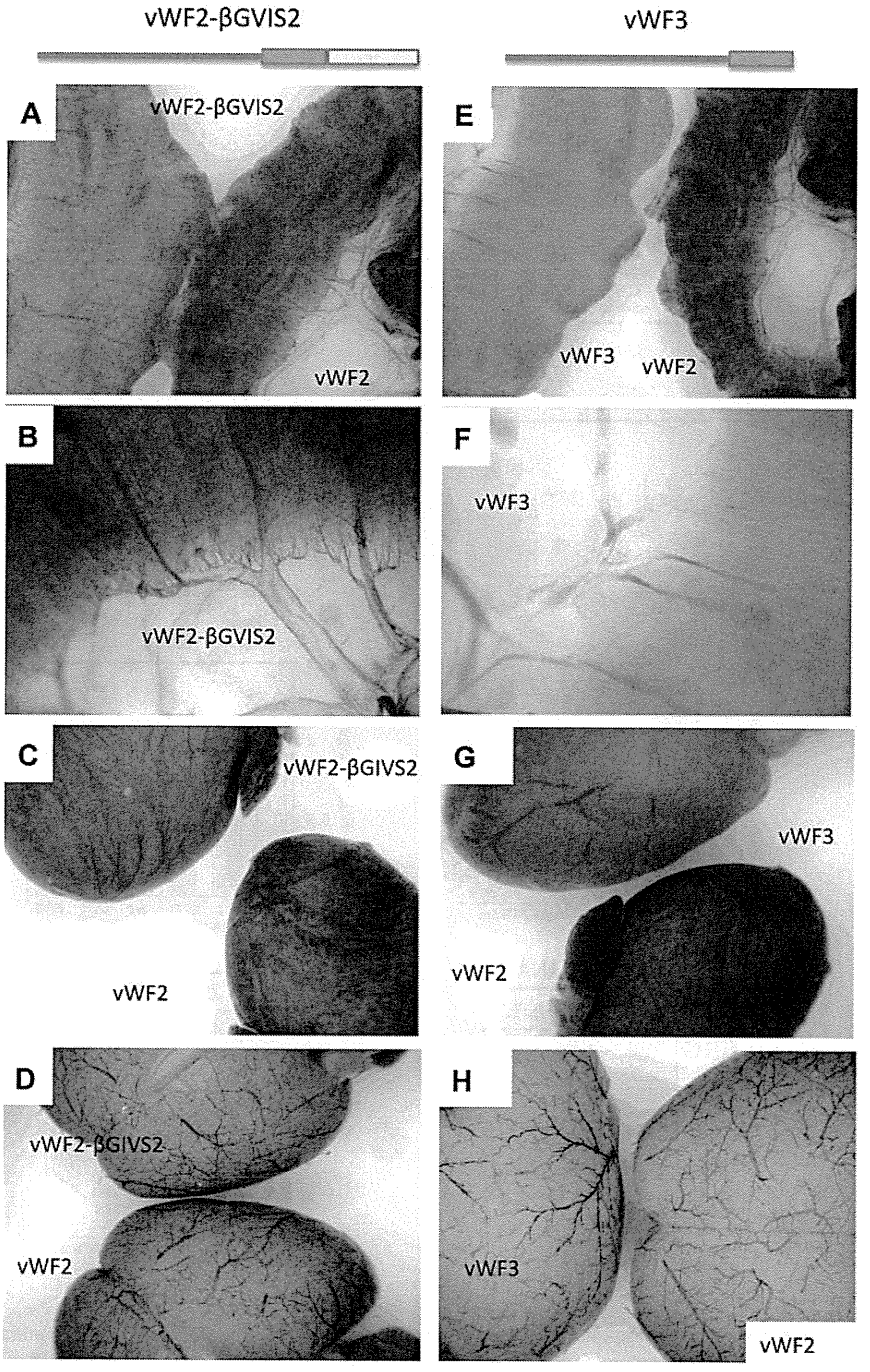

Figure 4. LacZ staining of diaphragm, heart and brain from *Hprt*-targeted mice carrying vWF2-lacZ, vWF3-lacZ, or vWF2-βGIVS2-lacZ. Diaphragms, hearts, and brains were harvested from 6- to 8-week-old F2 male *Hprt*-targeted mice carrying vWF2-lacZ (vWF sequences between −2182 and +1475), vWF3-lacZ (vWF sequences between −2182 and +246), or vWF2-βGIVS2-lacZ (vWF sequences between −2182 and +246 and intron 2 from the human β-globin gene) and processed in parallel for whole-mount staining with X-Gal. In panels A and E, the diaphragm from the vWF2-lacZ transgenic mouse is on the right, and the diaphragm from the vWF2-βGIVS2-lacZ or vWF3-lacZ mouse is on the left. Panels B and F are higher power images of vWF2-βGIVS2-lacZ and vWF3-lacZ diaphragms, respectively. In panel C, the vWF2-lacZ heart is on the bottom, and the vWF2-βGIVS2-lacZ heart is on the top. In panel G, the vWF2-lacZ heart is on the bottom, and the vWF3-lacZ heart is on the top. In panel D, the vWF2-lacZ brain is on the bottom, and the vWF2-βGIVS2-lacZ brain is on the top. In panel H, the vWF2-lacZ brain is on the right, and the vWF3-lacZ brain is on the left. In panels A through D, vWF2-βGIVS2-lacZ organs reveal a similar pattern (though lower absolute levels) of expression compared with vWF2-lacZ. In E-H, vWF3-lacZ organs show the X-Gal reaction product in brain but not heart or skeletal muscle. Whole-mount tissues were analyzed under a Nikon SMZ-U dissecting microscope, and microphotographs were collected using a Nikon Coolpix 8400 camera.

Finally, to determine the role of the ERG-binding site in mediating expression of the VWF promoter in vivo, we targeted the *Hprt* locus with the vWF2 promoter containing a mutation of the −56 ETS motif coupled to LacZ. Analysis of the resulting mice did not reveal detectable expression of β-galactosidase with the exception of occasional positive blood vessels in the hindbrain (Figure 6). Thus, the −56 ETS motif is necessary for vWF2 promoter activity in blood vessels of the heart and skeletal muscle.

Discussion

One feature of the endothelium that is often overlooked is its rich diversity of regional and organ-specific phenotypes. Endothelial cell heterogeneity has been described at the level of cell morphology, function, gene expression, and antigen composition. Endothelial cell phenotypes vary between different organs, between different segments of the vascular loop within the same organ, and between neighboring endothelial cells of the same organ and blood vessel type (reviewed by Aird[26]). In vivo proteomic approaches have revealed a striking array of vascular bed–specific phenotypes. For example, antibody and subfractionation strategies have been employed to generate monoclonal antibodies that specifically target the caveolae in one vascular bed or another.[27] Others have used phage display peptide libraries to select for peptides that home to specific vascular beds in vivo. These latter studies have uncovered a vascular address system that allows for site-specific targeting of

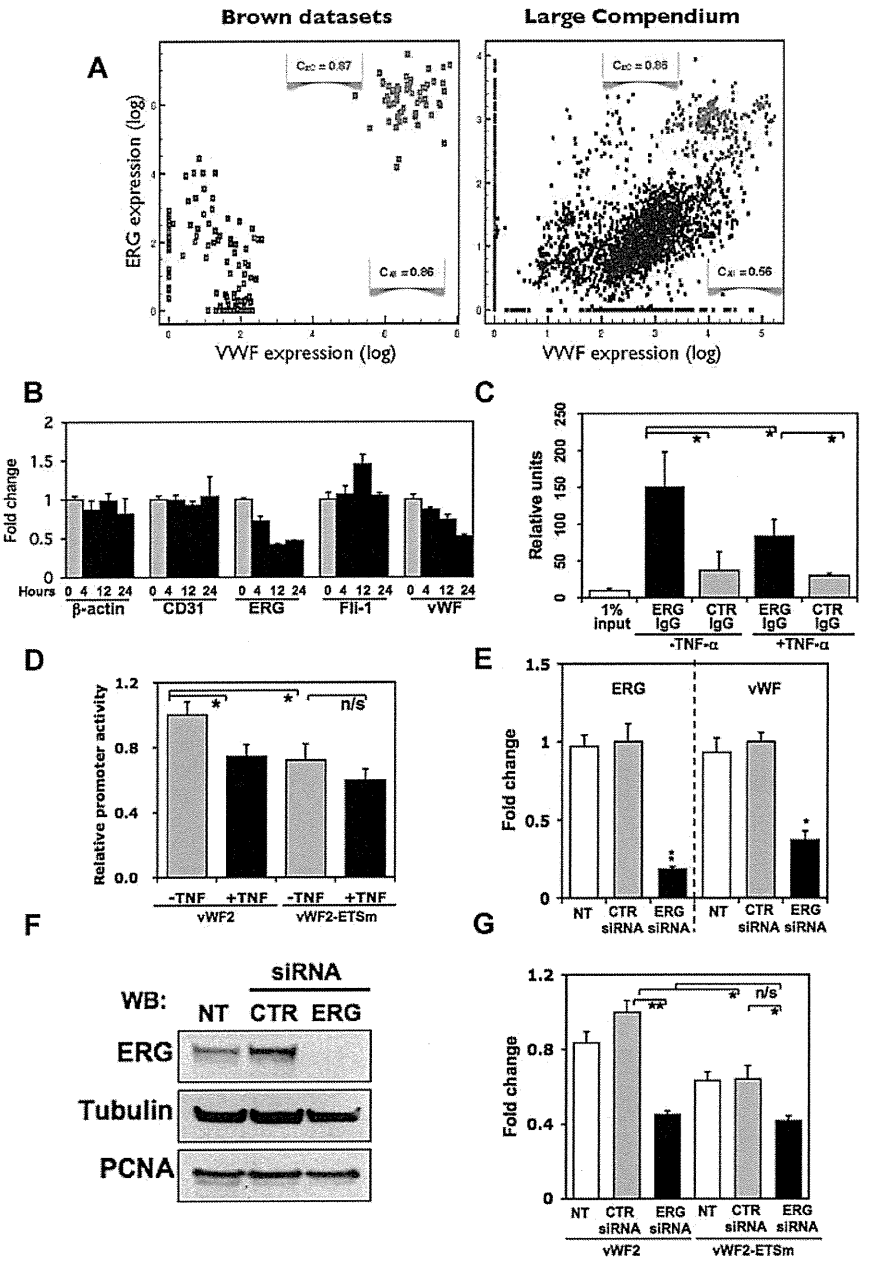

Figure 5. ERG binds to the −56 ETS motif. (A) VWF expression is shown as a function of ERG expression levels. Results are based on the Brown datasets (left) and our compendium of 5532 arrays (right). Red, endothelial cells; black, nonendothelial cells. (B) Quantitative real-time PCR analysis of β-actin, CD31, ERG, friend leukemia virus integration-1, and VWF in HUVECs treated with 20 ng/mL TNF-α for 0 (untreated control), 4, 12, or 24 hours. For each gene, expression is shown relative to control values. Data are expressed as mean + SD of 3 independent experiments. (C) ChIP assay was performed using HUVECs treated in the absence of presence of TNF-α for 12 hours. DNA was sheared, and the resulting DNA-protein complexes were immunoprecipitated in the absence or presence of antibodies to ERG or control IgG. Real-time PCR analysis was performed using the precipitated DNA fragments and primers for VWF proximal region, which included the −56 ETS site. (D) Transient transfection of vWF2-Luc or vWF2-ETSm-Luc in HUVECs treated in the absence or presence of TNF-α for 4 hours. The results show the mean + SD of luciferase light units (relative to vWF2 in untreated cells) obtained in triplicate from at least 3 independent experiments. $^*P < .05$. (E) HUVECs were either not transfected (NT) or transfected with control siRNA (CTR) or siRNA against ERG (ERG) and assayed for mRNA expression of ERG or VWF by real-time PCR. The results in E show the mean + SD of mRNA expression (relative to control siRNA-transfected cells) obtained in triplicate from 3 independent experiments. $^*P < .05$, relative to control siRNA. (F) Same HUVECs as described in E were assayed for ERG protein expression using Western blot. For loading control, the blot was stripped and reprobed with antibodies against tubulin and against the nuclear marker, proliferating cell nuclear antigen (PCNA). (G) Parallel plates of HUVECs used for mRNA and protein analysis in panels E and F were transiently transfected with vWF2-Luc or vWF2-ETSm-Luc. The results show the mean + SD of luciferase light units (relative to vWF2 in control siRNA-transfected cells) obtained in triplicate from at least 3 independent experiments. $^*P < .05$; $^{**}P < .01$; n/s, nonsignificant.

biologically active compounds, for example, to the endothelial lining of tumor blood vessels.[28]

The molecular basis of endothelial heterogeneity remains poorly defined. One approach to this problem is to study the mechanisms underlying differential gene regulation. Previous studies using standard transgenic mice have shown that most endothelial promoters contain information for expression in a subset of vascular beds in vivo.[12,29-36] In *Hprt*-targeted mice, different fragments of the VWF, FLT-1, endothelial nitric oxide synthase, and ROBO4 promoters have been shown to direct expression in distinct vascular beds.[8,37-39] Collectively, these data argue against the existence of a pan-endothelial "master regulator" and suggest that at least some endothelial genes are regulated by vascular bed–specific promoter modules.

The results of the current study provide compelling new evidence for such a mechanism in mediating VWF expression. Specifically, we have shown that DNA sequences between −843 and −620 contain information for expression of VWF in the capillary endothelium of the heart and skeletal muscle. Indeed, the finding that vWF2-Del3-lacZ mice (containing VWF sequences between −620 and +1475) and vWF2-$\Delta_{843\text{-}620}$-lacZ mice (containing VWF sequences between −2182 and +1475, but with an internal deletion of −843 to −620) lose expression in the capillaries of the heart and skeletal muscle indicates that the 224-bp region is necessary for site-specific expression. The −843 to −620 region does not appear to function as a classical enhancer because it failed (at least in the context of the larger −843 to −487 region) to confer microvascular expression in the heart and skeletal muscle when coupled to a minimal TK promoter.

Although we have examined a large number of organs in vWF2 and vWF2-$\Delta_{843\text{-}620}$-lacZ mice for LacZ expression, the survey is not exhaustive. Thus, we cannot exclude the possibility that the vWF2 promoter is active in other, yet unexplored vascular beds. This limitation does not detract from the main finding in the paper,

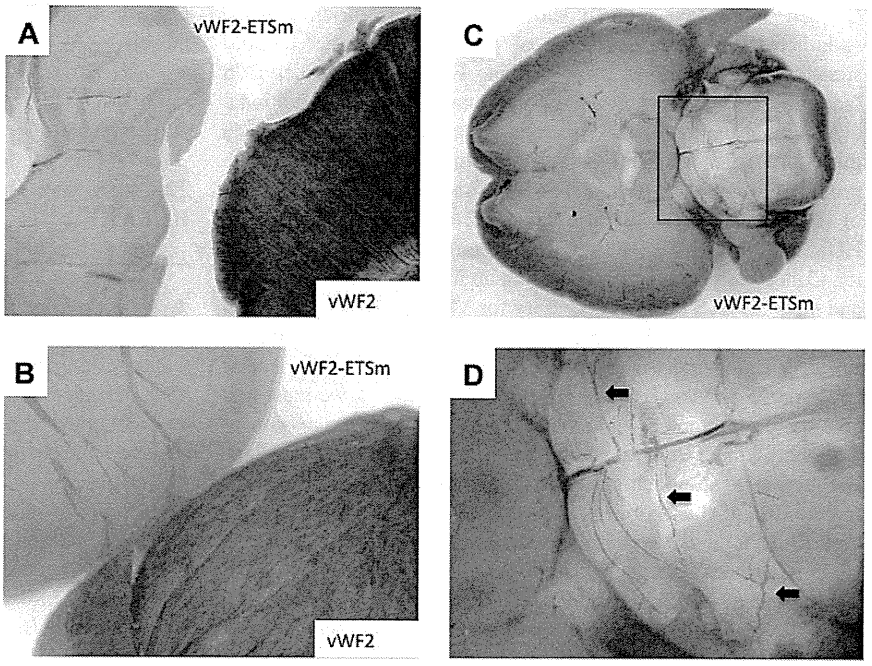

Figure 6. LacZ staining of diaphragm, heart, and brain from *Hprt*-targeted mice carrying vWF2-lacZ or vWF2-ETSm-lacZ. Diaphragms, hearts, and brains were harvested from 6- to 8-week-old F2 male *Hprt*-targeted mice carrying vWF2-lacZ or vWF2-ETSm-lacZ and processed in parallel for whole-mount staining with X-Gal. (A) The diaphragm from the vWF2-lacZ transgenic mouse is on the right, and the diaphragm from the vWF2-ETSm-lacZ mouse is on the left. (B) The vWF2-lacZ heart is on the bottom, and the vWF2-ETSm-lacZ heart is on the top. (C-D) The vWF2-ETSm-lacZ brain at low and high power, respectively (panel D is from the inset shown in panel C). Note the lack of detectable LacZ staining in skeletal muscle (diaphragm) and heart. Whole-mount tissues were analyzed under a Nikon SMZ-U dissecting microscope, and microphotographs were collected using a Nikon Coolpix 8400 camera. Arrows, LacZ-positive blood vessels in posterior brain.

namely that capillary endothelial expression in the heart and skeletal muscle is selectively lost in the vWF2-$\Delta_{843\text{-}620}$-lacZ mice.

The present data raise a fundamental question: what DNA sequences within this region are responsible for mediating promoter activity in such a limited subset of endothelial cells? To identify candidate regulatory elements, we used Multiz Alignment through the University of California Santa Cruz Genome Browser to compare the −843 to −620 region in the human promoter to similar sequences in the mouse and bovine VWF promoters. On the human promoter fragment, 5 TRANSFAC binding matrices were detected by MATCH, 3 of which, ZNF143, TAL1/TCF3 complex, and BCL6, were moderately conserved between all 3 species (supplemental Figure 13). Furthermore, 25 JASPAR matrix binding sites were also identified, 8 of which are conserved: 3 ETS1 sites, SP1, HOXA5, PDX1, PRRX2, and MZF1 (supplemental Figure 13). Given their location (between −843 and −620), each of these evolutionarily conserved sequences is a candidate for site-specific expression of VWF in the microvascular endothelium of heart and skeletal muscle. In transient transfections of HUVECs, the vWF2 and vWF2-$\Delta_{843\text{-}620}$ promoters demonstrate comparable activity, and VWF promoter activity is not induced by the addition of conditioned medium from primary rat cardiomyocytes (data not shown). To date, we have been unsuccessful in transiently transfecting primary mouse heart capillary endothelial cells. Thus, in the absence of an appropriate in vitro system, continued efforts to delineate the microvascular bed–specific DNA elements between −843 and −620 will rely on *Hprt*-locus targeting.

In addition to generating increased protein diversity through alternative splicing, many studies have shown that constitutively spliced introns are required for optimal gene expression. In some cases, the effect is mediated by *cis*-regulatory elements present in the native intron. Such a mechanism has been implicated for vascular endothelial growth factor receptor 2/FLK-1, TIE-2, GATA2, endoglin, and VWF (the latter involving DNA sequences in intron 51).[11-15] In other cases, gene expression enhancement occurs with native or non-native introns alike, suggesting a role for splicing per se. The mechanisms underlying splicing-mediated enhancement of gene expression are poorly understood but may involve increased transcription[16,17,40] and/or increased nuclear export of mRNA.[41]

The finding that the intron-less vWF3 promoter (−2182 to +246) lacked activity in the heart and skeletal muscle pointed to an important role of the promoter proximal intron in mediating expression in these vascular beds. However, the finding that the non-native second intron of the human β-globin gene could largely rescue expression of the −2182 to +246 promoter argues against a critical role for gene-specific regulatory elements in the VWF intron. Previous studies demonstrated that the second intron of the human β-globin gene rescued expression of a heterologous promoter when placed between the promoter and the cDNA but not when placed 3′ of the gene or 5′ of the promoter.[16,20] Thus, it seems unlikely that the β-globin intron is augmenting VWF expression by an enhancer-dependent mechanism. Rather, the data point to a requirement for intronic splicing. This is the first study of which we are aware to implicate a role for intronic splicing in the expression of an endothelial gene. More importantly, the observation that vWF3-lacZ expresses in the brain but not the heart or skeletal muscle suggests that the effects of splicing on gene expression vary between vascular beds, and thus may represent a novel mechanism of endothelial cell heterogeneity.

A mutation of the −56 ETS motif in the context of the vWF2 promoter resulted in complete loss of expression in the heart and skeletal muscle and significantly reduced expression in the brain. These findings implicate a critical role for the −56 ETS motif in mediating expression of VWF. Consensus ETS binding motifs have been identified within the promoters of several endothelial-restricted genes, including *VWF, FLT-1, TIE1, TIE2, FLK-1*, endothelial nitric oxide synthase, and vascular endothelial-cadherin.[42-46] Previous studies from our own group and others have demonstrated the functional relevance of ETS motifs in mediating endothelial gene expression of VWF using standard transgenic mice, *Hprt*-targeted mice, and by introducing a mutation into the endogenous promoter.[38,44,45,47,48] Various ETS family members have been implicated in the regulation of endothelial gene expression, including ELF, ETS-1, ETS-2, GABP, and ERG (reviewed by

Oettgen[49]). We have recently shown that ERG is enriched in the endothelium.[9] A previous study of the VWF promoter demonstrated that the −56 ETS motif binds ERG but not other ETS factors.[21] In the current study, we have provided additional evidence for the role of ERG in mediating expression of VWF via the −56 ETS motif. ChIP assays confirm binding of ERG to the proximal promoter region in HUVECs, and transient transfections of ERG-deficient HUVECs with vWF2 and of ERG-competent HUVECs with vWF2-ETSm revealed comparable promoter activity. Collectively, the data suggest that an interaction between ERG and the −56 ETS motif is necessary for VWF promoter activity in the vascular beds of the heart and skeletal muscle. The −56 ETS site may also be necessary for VWF expression in other vascular beds and/or megakaryocytes. To test this hypothesis, we must first identify the promoter regions that direct authentic expression of VWF throughout the vasculature and in megakaryocytes/platelets. An alternative approach would be to mutate the −56 ETS motif in the context of the endogenous mouse VWF locus as previously described for the *ROBO4* gene.[48]

In summary, we have shown that a 224-bp region of the VWF promoter (between −843 and −620) functions in conjunction with an ETS motif and an intron (ie, by splicing) to mediate gene expression in the capillary endothelium of the heart and skeletal muscle.

Acknowledgment

This work was supported by National Institutes of Health grant HL076540.

Authorship

Contribution: J.L., L.Y., G.M., E.R., L.J., D.B., K.C.S., Y.O., and T.M. designed and performed experiments and analyzed the data; P.O. designed experiments and analyzed the data; and W.C.A. designed and performed experiments, analyzed the data, and wrote the manuscript.

Conflict-of-interest disclosure: The authors declare no competing financial interests.

Correspondence: William C. Aird, Beth Israel Deaconess Medical Center, Molecular and Vascular Medicine, RW-663, 330 Brookline Ave, Boston, MA; e-mail: waird@bidmc.harvard.edu.

References

1. Yamamoto K, de Waard V, Fearns C, Loskutoff DJ. Tissue distribution and regulation of murine von Willebrand factor gene expression in vivo. *Blood.* 1998;92(8):2791-2801.
2. Guan J, Guillot PV, Aird WC. Characterization of the mouse von Willebrand factor promoter. *Blood.* 1999;94(10):3405-3412.
3. Janel N, Schwachtgen JL, Bakhshi MR, Barek L, Meyer D, Kerbiriou-Nabias D. Comparison of the 5′-flanking sequences of the human and bovine von Willebrand factor-encoding genes reveals alternation of highly homologous domains with species-specific Alu-type repeats. *Gene.* 1995; 167(1-2):291-295.
4. Mancuso DJ, Tuley EA, Westfield LA, et al. Structure of the gene for human von Willebrand factor. *J Biol Chem.* 1989;264(33):19514-19527.
5. Jahroudi N, Lynch DC. Endothelial-cell-specific regulation of von Willebrand factor gene expression. *Mol Cell Biol.* 1994;14(2):999-1008.
6. Aird WC, Jahroudi N, Weiler-Guettler H, Rayburn HB, Rosenberg RD. Human von Willebrand factor gene sequences target expression to a subpopulation of endothelial cells in transgenic mice. *Proc Natl Acad Sci U S A.* 1995;92(10):4567-4571.
7. Aird WC, Edelberg JM, Weiler-Guettler H, Simmons WW, Smith TW, Rosenberg RD. Vascular bed-specific expression of an endothelial cell gene is programmed by the tissue microenvironment. *J Cell Biol.* 1997;138(5):1117-1124.
8. Minami T, Donovan DJ, Tsai JC, Rosenberg RD, Aird WC. Differential regulation of the von Willebrand factor and Flt-1 promoters in the endothelium of hypoxanthine phosphoribosyltransferase-targeted mice. *Blood.* 2002;100(12):4019-4025.
9. Yuan L, Nikolova-Krstevski V, Zhan Y, et al. Antiinflammatory effects of the ETS factor ERG in endothelial cells are mediated through transcriptional repression of the interleukin-8 gene. *Circ Res.* 2009;104(9):1049-1057.
10. Liu J, Kanki Y, Okada Y, et al. A +220 GATA motif mediates basal but not endotoxin-repressible expression of the von Willebrand factor promoter in Hprt-targeted transgenic mice. *J Thromb Haemost.* 2009;7(8):1384-1392.
11. Kappel A, Ronicke V, Damert A, Flamme I, Risau W, Breier G. Identification of vascular endothelial growth factor (VEGF) receptor-2 (Flk-1) promoter/enhancer sequences sufficient for angioblast and endothelial cell-specific transcription in transgenic mice. *Blood.* 1999;93(12):4284-4292.
12. Schlaeger TM, Bartunkova S, Lawitts JA, et al. Uniform vascular-endothelial-cell-specific gene expression in both embryonic and adult transgenic mice. *Proc Natl Acad Sci U S A.* 1997; 94(7):3058-3063.
13. Kleinschmidt AM, Nassiri M, Stitt MS, et al. Sequences in intron 51 of the von Willebrand factor gene target promoter activation to a subset of lung endothelial cells in transgenic mice. *J Biol Chem.* 2008;283(5):2741-2750.
14. Khandekar M, Brandt W, Zhou Y, et al. A Gata2 intronic enhancer confers its pan-endothelia-specific regulation. *Development.* 2007;134(9):1703-1712.
15. Pimanda JE, Chan WY, Wilson NK, et al. Endoglin expression in blood and endothelium is differentially regulated by modular assembly of the Ets/Gata hemangioblast code. *Blood.* 2008; 112(12):4512-4522.
16. Palmiter RD, Sandgren EP, Avarbock MR, Allen DD, Brinster RL. Heterologous introns can enhance expression of transgenes in mice. *Proc Natl Acad Sci U S A.* 1991;88(2):478-482.
17. Brinster RL, Allen JM, Behringer RR, Gelinas RE, Palmiter RD. Introns increase transcriptional efficiency in transgenic mice. *Proc Natl Acad Sci U S A.* 1988;85(3):836-840.
18. Choi T, Huang M, Gorman C, Jaenisch R. A generic intron increases gene expression in transgenic mice. *Mol Cell Biol.* 1991;11(6):3070-3074.
19. Buchman AR, Berg P. Comparison of intron-dependent and intron-independent gene expression. *Mol Cell Biol.* 1988;8(10):4395-4405.
20. Collis P, Antoniou M, Grosveld F. Definition of the minimal requirements within the human beta-globin gene and the dominant control region for high level expression. *EMBO J.* 1990;9(1):233-240.
21. Schwachtgen JL, Janel N, Barek L, et al. Ets transcription factors bind and transactivate the core promoter of the von Willebrand factor gene. *Oncogene.* 1997;15(25):3091-3102.
22. Chi JT, Chang HY, Haraldsen G, et al. Endothelial cell diversity revealed by global expression profiling. *Proc Natl Acad Sci U S A.* 2003;100(19): 10623-10628.
23. Chi JT, Rodriguez EH, Wang Z, et al. Gene expression programs of human smooth muscle cells: tissue-specific differentiation and prognostic significance in breast cancers. *PLoS Genet.* 2007;3(9):1770-1784.
24. Chi JT, Wang Z, Nuyten DS, et al. Gene expression programs in response to hypoxia: cell type specificity and prognostic significance in human cancers. *PLoS Med.* 2006;3(3):e47.
25. McLaughlin F, Ludbrook VJ, Cox J, von Carlowitz I, Brown S, Randi AM. Combined genomic and antisense analysis reveals that the transcription factor Erg is implicated in endothelial cell differentiation. *Blood.* 2001;98(12):3332-3339.
26. Aird WC. Spatial and temporal dynamics of the endothelium. *J Thromb Haemost.* 2005;3(7): 1392-1406.
27. McIntosh DP, Tan XY, Oh P, Schnitzer JE. Targeting endothelium and its dynamic caveolae for tissue-specific transcytosis in vivo: a pathway to overcome cell barriers to drug and gene delivery. *Proc Natl Acad Sci U S A.* 2002;99(4):1996-2001.
28. Arap W, Haedicke W, Bernasconi M, et al. Targeting the prostate for destruction through a vascular address. *Proc Natl Acad Sci U S A.* 2002;99(3): 1527-1531.
29. Guillot PV, Guan J, Liu L, et al. A vascular bed-specific pathway. *J Clin Invest.* 1999;103(6):799-805.
30. Tsai JC, Liu L, Cooley BC, DiChiara MR, Topper JN, Aird WC. The Egr-1 promoter contains information for constitutive and inducible expression in transgenic mice. *Faseb J.* 2000;14(13):1870-1872.
31. Seki T, Hong KH, Yun J, Kim SJ, Oh SP. Isolation of a regulatory region of activin receptor-like kinase 1 gene sufficient for arterial endothelium-specific expression. *Circ Res.* 2004;94(8):e72-77.
32. Porat RM, Grunewald M, Globerman A, et al. Specific induction of tie1 promoter by disturbed flow in atherosclerosis-prone vascular niches and flow-obstructing pathologies. *Circ Res.* 2004;94(3):394-401.
33. Schlaeger TM, Qin Y, Fujiwara Y, Magram J, Sato TN. Vascular endothelial cell lineage-specific promoter in transgenic mice. *Development.* 1995; 121(4):1089-1098.
34. Gory S, Vernet M, Laurent M, Dejana E, Dalmon J, Huber P. The vascular endothelial-cadherin

promoter directs endothelial-specific expression in transgenic mice. *Blood.* 1999;93(1):184-192.

35. Harats D, Kurihara H, Belloni P, et al. Targeting gene expression to the vascular wall in transgenic mice using the murine preproendothelin-1 promoter. *J Clin Invest.* 1995;95(3):1335-1344.
36. Pimanda JE, Chan WY, Donaldson IJ, Bowen M, Green AR, Gottgens B. Endoglin expression in the endothelium is regulated by Fli-1, Erg, and Elf-1 acting on the promoter and a -8-kb enhancer. *Blood.* 2006;107(12):4737-4745.
37. Guillot PV, Liu L, Kuivenhoven JA, Guan J, Rosenberg RD, Aird WC. Targeting of human eNOS promoter to the Hprt locus of mice leads to tissue-restricted transgene expression. *Physiol Genomics.* 2000;2(2):77-83.
38. Okada Y, Yano K, Jin E, et al. A three-kilobase fragment of the human Robo4 promoter directs cell type-specific expression in endothelium. *Circ Res.* 2007;100(12):1712-1722.
39. Jin E, Liu J, Suehiro J, et al. Differential roles for ETS, CREB, and EGR binding sites in mediating VEGF receptor 1 expression in vivo. *Blood.* 2009; 114(27):5557-5566.
40. Furger A, O'Sullivan JM, Binnie A, Lee BA, Proudfoot NJ. Promoter proximal splice sites enhance transcription. *Genes Dev.* 2002;16(21): 2792-2799.
41. Valencia P, Dias AP, Reed R. Splicing promotes rapid and efficient mRNA export in mammalian cells. *Proc Natl Acad Sci U S A.* 2008;105(9): 3386-3391.
42. Dube A, Akbarali Y, Sato TN, Libermann TA, Oettgen P. Role of the Ets transcription factors in the regulation of the vascular-specific Tie2 gene. *Circ Res.* 1999;84(10):1177-1185.
43. Dube A, Thai S, Gaspar J, et al. Elf-1 is a transcriptional regulator of the Tie2 gene during vascular development. *Circ Res.* 2001;88(2):237-244.
44. Iljin K, Dube A, Kontusaari S, et al. Role of ets factors in the activity and endothelial cell specificity of the mouse Tie gene promoter. *FASEB J.* 1999;13(2):377-386.
45. Minami T, Kuivenhoven JA, Evans V, Kodama T, Rosenberg RD, Aird WC. Ets motifs are necessary for endothelial cell-specific expression of a 723-bp Tie-2 promoter/enhancer in Hprt targeted transgenic mice. *Arterioscler Thromb Vasc Biol.* 2003;23(11):2041-2047.
46. Gory S, Dalmon J, Prandini MH, Kortulewski T, de Launoit Y, Huber P. Requirement of a GT box (Sp1 site) and two Ets binding sites for vascular endothelial cadherin gene transcription. *J Biol Chem.* 1998;273(12):6750-6755.
47. De Val S, Anderson JP, Heidt AB, Khiem D, Xu SM, Black BL. Mef2c is activated directly by Ets transcription factors through an evolutionarily conserved endothelial cell-specific enhancer. *Dev Biol.* 2004;275(2):424-434.
48. Okada Y, Jin E, Nikolova-Krstevski V, et al. A GABP-binding element in the Robo4 promoter is necessary for endothelial expression in vivo. *Blood.* 2008.
49. Oettgen P. Regulation of vascular inflammation and remodeling by ETS factors. *Circ Res.* 2006; 99(11):1159-1166.